[redacted]

NAVY DEPARTMENT

THE DAVID W. TAYLOR MODEL BASIN

WASHINGTON 7, D.C.

HYDRODYNAMIC FORCES AND MOMENTS ACTING ON A SLENDER BODY OF REVOLUTION MOVING UNDER A REGULAR TRAIN OF WAVES

by

William E. Cummins

[redacted]

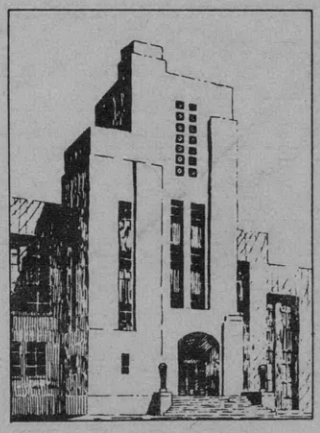

December 1954

[redacted]

Report 910

HYDRODYNAMIC FORCES AND MOMENTS ACTING ON A SLENDER BODY OF REVOLUTION MOVING UNDER A REGULAR TRAIN OF WAVES

by

William E. Cummins

December 1954

Report 910

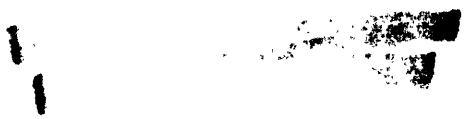

TABLE OF CONTENTS

NOTATION

A	Area of a transverse section
A_0	Area of midship section
$\mathbf{A}_i$	Vector strength of a discrete doublet
$\mathcal{A}(\xi)$	Dimensionless sectional area: $\mathcal{A}(\xi) = \frac{A(\xi)}{A_0}$
a	Radius of a transverse section
a_0, a_1 b_0, b_1	Integrals defined in Equations [65] to [68]
$C_{f,\,x}$, etc.	$F_x/\rho g A_0 L$, etc.
$C_{f,\,x;\,\max}$	Maximum value of $C_{f,\,x}$ during one cycle
$C_{m,\,y}$, etc.	$M_y/\rho g A_0 L^2$, etc.
$C_{m,\,y;\,\max}$	Maximum value of $C_{m,\,y}$ during one cycle
c	Celerity of wave; $c^2 = g\lambda/2\pi$
c_i	Fourier coefficients for expansion of $\mathcal{A}(\xi)$ in Legendre polynomials
D	Function defined in Equation [82]
d_{ij}	Coefficients used in evaluating $\{c_i\}$ numerically
$\mathbf{F}$	Total hydrodynamic force
$\mathbf{F}_l$	"Lagally" force; the portion of the hydrodynamic force which is independent of the rate of change of the flow
$\mathbf{F}_t$	Portion of the hydrodynamic force which is directly dependent upon the rate of change of the flow
$_c$, $F_{l,\,x}$, etc.	Components of $\mathbf{F}$, $\mathbf{F}_l$ in x-direction, etc.
$\mathcal{F}$	Froude number, $\mathcal{F} = V/\sqrt{gL}$
G	Function defined in Equation [83]
g	Acceleration due to gravity
H	Depth of centerline of body below the calm free surface
h	Height of waves (double amplitude)
$\mathbf{i}, \mathbf{j}, \mathbf{k}$	Unit vectors in x-, y-, z- directions
L	Length of body

$\mathbf{M}$	Total hydrodynamic moment
$\mathbf{M}_l$	"Lagally" moment; the portion of the hydrodynamic moment which is independent of the rate of change of the flow
$\mathbf{M}_t$	Portion of the hydrodynamic moment which is directly dependent upon the rate of change of the flow
$\mathbf{M}_{t,w}$, $\mathbf{M}_{t,s}$	Portions of $\mathbf{M}_t$ which are caused by the moving wave system and the changing singularity system, respectively
M_y, M_z	Components of $\mathbf{M}$ about the y-and z-axes
$\mathbf{n}$	Unit vector, normal to the surface of the body and directed inward
$P_i(\xi)$	Legendre polynomials
$\mathbf{q}_w$	Fluid velocity due to wave system, relative to body
$\mathbf{R}_i$	Position vector, referred to point $x' = x_i'$ on axis of body (see Figure 2)
$\mathbf{r}$	Position vector, referred to midpoint of the axis of the body
S_n	Spherical Bessel functions
s	Arc length along the profile of the body
t	Time
T_n	See Equation [76]
u, v, w	Fluid velocities in x-, y-, z-directions due to the wave train, relative to fixed axes.
u', v', w'	Fluid velocities relative to axes moving with the body
V	Velocity of the body along its axis
x, y, z	Coordinates referred to fixed system of axes
x', y', z'	Coordinates referred to axes moving with the body
α	See Figure 2
β	Angle between x-axis and a line normal to the wave crests (see Figure 1)
γ	$\pi L/\lambda$
ϵ_1	Angle determing the phase relationships of the forces (see Equation [84])
ϵ_2	Angle determing the phase relationships of the moments (see Equation [85])
η	Surface elevation of the wave from the calm water position
θ	See Figure 2
λ	Wavelength
μ	Vector strength of the axial doublet distribution
μ_x, μ_y, μ_z	Components of μ in x-, y-, z-directions

ξ	Dimensionless length along axis of the body; $\xi = \frac{2x'}{L}$
ρ	Mass density of water
Φ	Total velocity potential of flow relative to moving axes
ϕ_s	Velocity potential due to singularity system
ϕ_w, ϕ_w'	Velocity potential of flow due to wave train, referred to stationary and moving axes
ψ	See Equations [1] and [9]
ω	Frequency of encounter; $\omega = \frac{2\pi}{\lambda}(V \cos \beta - c)$

ABSTRACT

The hydrodynamic forces and moments acting on a slender body of revolution are found for the case in which the body is moving with a constant linear velocity under a sinusoidal train of waves oblique to the course of the body. The analysis makes use of a representation of the body by a system of singularities, and the dynamic effects are evaluated by means of the methods developed in TMB Report 780. The forces and moments are given explicitly as functions of the sectional-area curve of the body. Three illustrative examples are worked out, including a case in which there is no analytic expression available for the sectional-area curve.

INTRODUCTION

The theoretical determination of the forces and moments on a body due to waves on a free surface is one of the outstanding problems of hydromechanics and is of considerable practical as well as theoretical interest. The case in which the waves are generated by the body has been extensively studied. The case in which the surface is independently disturbed by a train of waves has received much less attention, but it is probably of greater importance in naval architectural applications since this case is closely tied up with seaworthiness.

The usual method for estimating the effects due to a wave train is based on the Froude-Krylov assumption,[1] which considers the pressure variation due to the structure of the wave but neglects the dynamics of the flow around the body. For submerged bodies, this assumption is known to be quite inaccurate, and a solution which takes account of the boundary condition at the surface of the body is highly desirable.

In the present report, such an analysis is carried out for a slender body of revolution. The body is represented approximately by a system of singularities distributed along its axis, and the forces and moments are determined by means of an extension of Lagally's theorem developed by the author in a previous report.[2] A detailed computational procedure is outlined for computing the forces and moments in terms of the sectional-area curve of the body. Although the derivation is for a body of revolution, the method may be used for other slender bodies in which the cross sections depart somewhat from circular, with the expectation that the answer will at least be correct in order of magnitude.

The principal limitations on the analysis are that the fineness ratio of the body be large and that the ratio of the wavelength to body diameter also be large. This latter restriction is not serious, since the forces and moments are usually negligible for wavelengths less than half the body length. The limitation on fineness ratio will be relaxed somewhat in a report to appear shortly in which a more precise analysis is carried out for the particular case of the spheroid.[3]

---

[1]References are listed on page 33.

BOUNDARY CONDITIONS

The body of revolution is considered to be horizontal, with its axis at a depth H below the calm position of the free surface, and to be moving along its axis with the constant velocity V. We shall make use of two systems of coordinates, one fixed in space and one fixed with respect to the body. The coordinates referred to the fixed axes will be x, y, z, and the coordinates referred to the moving axes will be x', y', z'. Both systems are selected with the x axes parallel to the axis of the body and the z axis positive upward. The origins will be in the calm free surface.

The free surface is considered to be disturbed by a regular train of waves of length λ, height h, and celerity c. In linearized wave theory, the flow due to such a wave train in deep water satisfies the velocity potential, referred to the stationary axes:

$$\phi_w = \frac{hc}{2} e^{2\pi z/\lambda} \cos \psi \qquad [1]$$

where

$$\psi = \frac{2\pi}{\lambda} (x \cos \beta + y \sin \beta - ct)$$

and β is the angle between the x-axis and a line normal to the crests (see Figure 1). We will adopt the convention that the positive x-direction is selected so that $-\frac{\pi}{2} < \beta \leq +\frac{\pi}{2}$. Following seas will then correspond to $\beta = 0$, $V > 0$, while head seas will correspond to $\beta = 0$, $V < 0$. The wave celerity is a function of the wavelength

$$c^2 = \frac{g\lambda}{2\pi} \qquad [2]$$

and the fluid velocities are

$$u = -\frac{\partial \phi_w}{\partial x} = \frac{\pi hc \cos \beta}{\lambda} e^{2\pi z/\lambda} \sin \psi \qquad [3]$$

$$v = -\frac{\partial \phi_w}{\partial y} = \frac{\pi hc \sin \beta}{\lambda} e^{2\pi z/\lambda} \sin \psi \qquad [4]$$

$$w = -\frac{\partial \phi_w}{\partial z} = -\frac{\pi hc}{\lambda} e^{2\pi z/\lambda} \cos \psi \qquad [5]$$

The surface elevation is given by

$$\eta = \frac{h}{2} \sin \psi \qquad [6]$$

The relations between the moving and stationary coordinates are

$$x' = x - Vt, \quad y' = y, \quad z' = z \tag{7}$$

The flow with respect to the moving system will then satisfy the potential

$$\phi_w' = \frac{hc}{2} e^{2\pi z'/\lambda} \cos \psi + Vx' \tag{8}$$

where

$$\psi = \frac{2\pi}{\lambda}[x' \cos \beta + y' \sin \beta + (V \cos \beta - c)t] \tag{9}$$

The relative fluid velocities will be

$$u' = u - V, \quad v' = v, \quad w' = w \tag{10}$$

The force and moment will be evaluated with respect to the moving system, as if the relative velocities were the absolute velocities. The values so obtained will be correct, since these axes are not accelerating.[2]

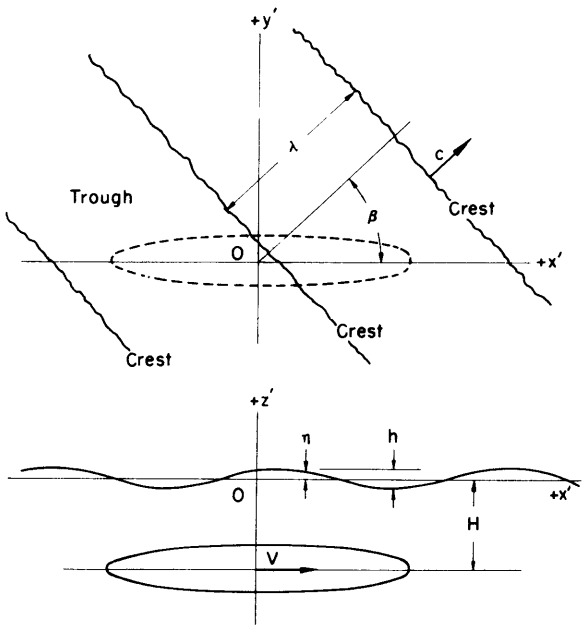

Figure 1

SINGULARITY SYSTEM

In order to set up an approximate singularity system for the representation of the body, we assume that over any short length of the body, the flow which would exist if the body were not present is approximately uniform. This implies that the diameter of the body is small in comparison with the wavelength. We then consider this flow to be resolved into components parallel to each of the axes and establish singularity systems such that the boundary condition at the surface of the body is satisfied for each component.

First, consider the transverse components. The procedure used by Pond in the study of the moment acting on a body of revolution moving under a calm free surface will be followed.[4] Here, the restriction to slender bodies enters, since it is assumed that over any short length the body can be considered cylindrical. The doublet distribution along the axis can then be approximated from two-dimensional theory:

$$\mu_y(x) = -\frac{1}{2}a^2 v' = -\frac{1}{2}a^2 v \qquad [11]$$

$$\mu_z(x) = -\frac{1}{2}a^2 w' = -\frac{1}{2}a^2 w \qquad [12]$$

where a is the radius of the body and μ_y and μ_z are the strengths of distributions of three-dimensional doublets with their axes parallel to the y- and z-axes, respectively.

For the axial component of the flow, we make use of the well-known Munk formula [5]

$$\mu_x = -\frac{1}{4}a^2 V_s$$

This distribution of doublets oriented parallel to the axis approximately represents a slender body in a uniform axial stream of velocity V_s. In the present case we have assumed that the axial component of the stream velocity u' is nearly constant over any short length, so we use a modified distribution

$$\mu_x(x) = -\frac{1}{4}a^2 u' = \frac{1}{4}a^2 (V - u) \qquad [13]$$

It is convenient to represent these three doublet distributions as components of a single distribution whose strength is the vector quantity

$$\boldsymbol{\mu} = \mu_x \mathbf{i} + \mu_y \mathbf{j} + \mu_z \mathbf{k} \qquad [14]$$

Using this distribution, we proceed to find the force and moment by means of the extended Lagally theorem. Since the distributions are correct only to the first order and since we are using a linearized theory, we are justified in dropping all terms of order higher than the first (e.g., terms containing u^2, v^2, uv, etc).

To be complete, we should also consider the effect on the body due to the waves caused by the singularities, that is, the waves due to the presence of the body. This we shall not attempt. The distribution μ_x will generate a wave system which, to the first order, is independent of the regular train of waves and is essentially identical with the wave system generated by the body moving under a calm surface. The moment for this condition has been discussed by Pond.[4] The distributions μ_y and μ_z will cause waves of higher order, which will be neglected.

THE HYDRODYNAMIC FORCE

In a time-varying flow, the net hydrodynamic force acting on a body is the sum of the usual Lagally force as evaluated from the instantaneous magnitudes of the singularities and a force which exists because the flow is changing.[2] If a body is represented by a system of discrete doublets with the vector strengths $\mathbf{A}_1$, $\mathbf{A}_2$, $\mathbf{A}_3$, ... the net force is given by

$$\mathbf{F} = \sum_i (\mathbf{F}_l + \mathbf{F}_t)_i \qquad [15]$$

where

$$(\mathbf{F}_l)_i = -4\pi\rho\ (\mathbf{A}_i \cdot \nabla)\ \mathbf{q}_w(i) \qquad [16]$$

$$(\mathbf{F}_t)_i = -4\pi\rho\ \frac{d\mathbf{A}_i}{dt} \qquad [17]$$

and

$$\mathbf{q}_w = u'\mathbf{i} + v'\mathbf{j} + w'\mathbf{k} \qquad [18]$$

(i.e., the velocity which would exist at the location of the doublet if the body were not present). For continuous distributions, the summation in Equation [15] becomes an integration. In the present case,

$$d\mathbf{F} = d\mathbf{F}_l + d\mathbf{F}_t \qquad [19]$$

where

$$d\mathbf{F}_l = -4\pi\rho \left(\mu_x \frac{\partial}{\partial x'} + \mu_y \frac{\partial}{\partial y'} + \mu_z \frac{\partial}{\partial z'}\right) \mathbf{q}_w\, dx' \qquad [20]$$

$$d\mathbf{F}_t = -4\pi\rho \left(\frac{\partial \mu_x}{\partial t}\,\mathbf{i} + \frac{\partial \mu_y}{\partial t}\,\mathbf{j} + \frac{\partial \mu_z}{\partial t}\,\mathbf{k}\right) dx' \qquad [21]$$

The partial derivatives appearing in these equations can be written

$$\frac{\partial \mu_x}{\partial t} = -\frac{1}{4}a^2 \frac{\partial u}{\partial t} = -\frac{a^2\pi^2 hc \cos\beta}{2\lambda^2}(V\cos\beta - c)\, e^{-2\pi H/\lambda} \cos\psi$$

$$= \frac{a^2\pi \cos\beta}{2\lambda}(V\cos\beta - c)w \qquad [22]$$

$$\frac{\partial \mu_y}{\partial t} = -\frac{1}{2}a^2 \frac{\partial v}{\partial t} = \frac{a^2\pi \sin\beta}{\lambda}(V\cos\beta - c)w \qquad [23]$$

$$\frac{\partial \mu_z}{\partial t} = -\frac{1}{2}a^2 \frac{\partial w}{\partial t} = -\frac{a^2\pi}{\lambda}\frac{(V\cos\beta - c)}{\cos\beta}u \qquad [24]$$

$$\frac{\partial u'}{\partial x'} = -\frac{2\pi\cos^2\beta}{\lambda}w, \qquad \frac{\partial u'}{\partial y'} = -\frac{2\pi\sin\beta\cos\beta}{\lambda}w, \qquad \frac{\partial u'}{\partial z} = \frac{2\pi}{\lambda}u \qquad [25]$$

$$\frac{\partial v'}{\partial x'} = -\frac{2\pi \sin\beta \cos\beta}{\lambda} w, \qquad \frac{\partial v'}{\partial y'} = -\frac{2\pi \sin^2\beta}{\lambda} w, \qquad \frac{\partial v'}{\partial z'} = \frac{2\pi}{\lambda} v \qquad [26]$$

$$\frac{\partial w'}{\partial x'} = \frac{2\pi}{\lambda} u, \qquad \frac{\partial w'}{\partial y'} = \frac{2\pi}{\lambda} v, \qquad \frac{\partial w'}{\partial z'} = \frac{2\pi}{\lambda} w \qquad [27]$$

Considering terms of the first order only, we have for the axial component of the force acting on a differential length

$$dF_{l,x} = \frac{2\pi^2}{\lambda} \rho a^2 V w \cos^2\beta \, dx' \qquad [28]$$

$$dF_{t,x} = -\frac{2\pi^2}{\lambda} \rho a^2 \cos\beta \, (V \cos\beta - c) \, w \, dx' \qquad [29]$$

so

$$dF_x = \frac{2\pi^2}{\lambda} \rho a^2 c w \cos\beta \, dx' = -\frac{\pi}{\lambda} \rho A g h \cos\beta \, e^{-2\pi H/\lambda} \cos\psi \, dx' \qquad [30]$$

where A is the sectional area. Thus, to the first order, the amplitude of the oscillating axial force is independent of the speed of advance of the body.

The differential side forces are

$$dF_{l,y} = \frac{2\pi^2}{\lambda} \rho a^2 V w \sin\beta \cos\beta \, dx' \qquad [31]$$

$$dF_{t,y} = -\frac{4\pi^2}{\lambda} \rho a^2 \sin\beta \, (V \cos\beta - c) \, w \, dx' \qquad [32]$$

and

$$dF_y = -\frac{2\pi}{\lambda} \rho A g h \sin\beta \left(1 - \frac{V \cos\beta}{2c}\right) e^{-2\pi H/\lambda} \cos\psi \, dx' \qquad [33]$$

The differential vertical forces are

$$dF_{l,z} = \frac{-2\pi^2}{\lambda} \rho a^2 V u \, dx' \qquad [34]$$

$$dF_{t,z} = \frac{4\pi^2}{\lambda \cos\beta} \rho a^2 (V \cos\beta - c) \, u \, dx' \qquad [35]$$

and

$$dF_z = -\frac{2\pi}{\lambda}\rho Agh\left(1 - \frac{V\cos\beta}{2c}\right)e^{-2\pi H/\lambda}\sin\psi\, dx' \qquad [36]$$

The total forces are then

$$F_x = -\frac{\pi\rho gh}{\lambda}\cos\beta\, e^{-2\pi H/\lambda}\int_{-L/2}^{+L/2} A\cos\psi\, dx' \qquad [37]$$

$$F_y = -\frac{2\pi\rho gh}{\lambda}\left(1 - \frac{V\cos\beta}{2c}\right)\sin\beta\, e^{-2\pi H/\lambda}\int_{-L/2}^{+L/2} A\cos\psi\, dx' \qquad [38]$$

$$F_z = \frac{-2\pi\rho gh}{\lambda}\left(1 - \frac{V\cos\beta}{2c}\right)e^{-2\pi H/\lambda}\int_{-L/2}^{+L/2} A\sin\psi\, dx' \qquad [39]$$

where $+L/2$ and $-L/2$ designate the ends of the body.

THE HYDRODYNAMIC MOMENT

Analogously to the force, the net moment acting on a body in a time-varying stream is also equal to the sum of the Lagally moment determined from the instantaneous strengths of the singularities and a moment due to the changing flow. In the case of the moment however, this latter component is given in terms of a surface integral. The moment can be written

$$\mathbf{M} = \mathbf{M}_l + \mathbf{M}_t \qquad [40]$$

where

$$\mathbf{M}_l = \sum_i (\mathbf{r}\times\mathbf{F}_l)_i + 4\pi\rho\sum_i (\mathbf{q}_w\times\mathbf{A})_i \qquad [41]$$

$$\mathbf{M}_t = \rho\frac{d}{dt}\int_S \Phi\,(\mathbf{r}\times\mathbf{n})\, d\sigma \qquad [42]$$

$\mathbf{r}$ is the position vector of a point referred to the center of moments, $\mathbf{n}$ is the inwardly directed unit vector normal to the surface of the body, and $\Phi = \phi_w' + \phi_s$ is the total velocity potential (wave train plus singularity system). The integration in Equation [42] is taken over the surface of the body, so $d\sigma$ is a differential surface element. We take the midpoint of the axis of the body as the center of moments.

The Lagally moment is easily obtained. Since

$$\mathbf{q}_w\times\mu = [v\mu_z - w\mu_y]\mathbf{i} + [w\mu_x - (u-V)\mu_z]\mathbf{j} + [(u-V)\mu_y - v\mu_x]\mathbf{k}$$

$$= \frac{1}{4}a^2(u-V)(w\mathbf{j} - v\mathbf{k})$$

$$\doteq -\frac{1}{4}a^2V(w\mathbf{j} - v\mathbf{k})$$

we have

$$d\mathbf{M}_l = -(x' dF_{l,z} + \pi\rho a^2 V w\, dx')\mathbf{j} + (x' dF_{l,y} + \pi\rho a^2 V v\, dx')\mathbf{k}$$
$$= \pi\rho a^2 V\left[\left(\frac{2\pi}{\lambda} ux' - w\right)\mathbf{j} + \left(\frac{2\pi}{\lambda} wx' \sin\beta\cos\beta + v\right)\mathbf{k}\right] dx' \qquad [43]$$

To evaluate the surface integral in Equation [42], we use the relations

$$\mathbf{n} = -\mathbf{i}\sin\alpha - \cos\alpha\,(\mathbf{j}\cos\theta + \mathbf{k}\sin\theta) \qquad [44]$$

$$\mathbf{r} = x'\mathbf{i} + a(\mathbf{j}\cos\theta + \mathbf{k}\sin\theta) \qquad [45]$$

where the angles α and θ are defined in Figure 2. Then

$$\mathbf{r}\times\mathbf{n} = (x'\cos\alpha - a\sin\alpha)(\mathbf{j}\sin\theta - \mathbf{k}\cos\theta)$$
$$= x'\cos\alpha\left(1 - \frac{a\sin\alpha}{x'\cos\alpha}\right)(\mathbf{j}\sin\theta - \mathbf{k}\cos\theta) \qquad [46]$$

For slender bodies, α is small except near the ends, but even for a body as blunt as a circular cylinder with hemispherical ends (see Figure 3)

$$\frac{a\sin\alpha}{x'\cos\alpha} = \frac{a\tan\alpha}{x'} = \frac{AB}{A0} \leq \frac{2a(0)}{L}$$

Therefore, we may use the approximate formula

$$\mathbf{r}\times\mathbf{n} \doteq x'\cos\alpha\,(\mathbf{j}\sin\theta - \mathbf{k}\cos\theta) \qquad [46a]$$

Then

$$\mathbf{M}_t = \rho\frac{d}{dt}\int_S\int \Phi\, ax'(\mathbf{j}\sin\theta - \mathbf{k}\cos\theta)\cos\alpha\, d\theta\, ds$$

where ds is a differential arc length along the profile. Since $\cos\alpha\, ds = dx'$,

$$\mathbf{M}_t = \rho\frac{d}{dt}\int_{-L/2}^{+L/2} ax'\int_0^{2\pi}\Phi(\mathbf{j}\sin\theta - \mathbf{k}\cos\theta)\, d\theta\, dx' \qquad [47]$$

The moment for a differential length is

$$d\mathbf{M}_t = \rho a x'\left[\frac{d}{dt}\int_0^{2\pi}(\phi_w' + \phi_s)(\mathbf{j}\sin\theta - \mathbf{k}\cos\theta)d\theta\right] dx' \qquad [48]$$

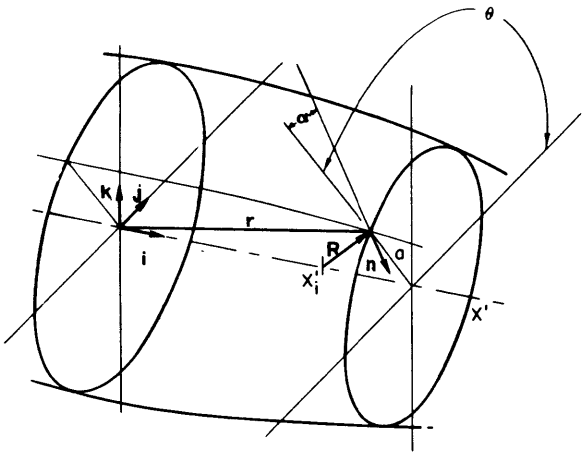

Figure 2

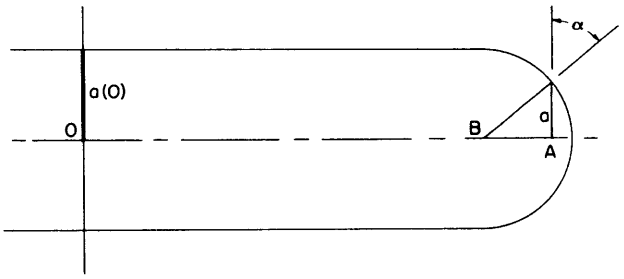

Figure 3

The contributions of ϕ_w' and ϕ_s will be evaluated separately. Expanding the potential ϕ_w' in a Taylor series about a point on the axis, the value at a point $(x', a\cos\theta, a\sin\theta - H)$ on the surface of the body is, (to the first order)

$$\phi_w'(x', a\cos\theta, a\sin\theta - H) = \phi_w'(x', 0, -H) + a\cos\theta\,\frac{\partial\phi_w'}{\partial y} + a\sin\theta\,\frac{\partial\phi_w'}{\partial z}$$

$$= \phi_w'(x', 0, -H) - a(v\cos\theta + w\sin\theta) \qquad [49]$$

Substituting in Equation [48] and integrating

$$d\mathbf{M}_{t,w} = -\pi\rho a^2 x'\left(\frac{\partial w}{\partial t}\mathbf{j} - \frac{\partial v}{\partial t}\mathbf{k}\right)dx'$$

$$= -\frac{2\pi^2}{\lambda}\rho a^2 x'(V\cos\beta - c)\left(\frac{u}{\cos\beta}\mathbf{j} + w\sin\beta\,\mathbf{k}\right)dx' \qquad [50]$$

Now considering the potential due to the singularity system, the distribution due to μ_x will contribute nothing to $d\mathbf{M}_t$, since it is axially symmetric and the integral with respect to θ will vanish. The remainder of the potential due to the singularity system is

$$\phi_s^*(x', a\cos\theta, a\sin\theta - H) = \int_{-L/2}^{+L/2} \frac{\mathbf{R}_i \cdot [\mu_y(x_i')\mathbf{j} + \mu_z(x_i')\mathbf{k}]}{R_i^3}\,dx_i'$$

$$= a\int_{-L/2}^{+L/2} \frac{\mu_y\cos\theta + \mu_z\sin\theta}{R_i^3}\,dx_i' \qquad [51]$$

where

$$\mathbf{R}_i = (x' - x_i')\,\mathbf{i} + a\cos\theta\,\mathbf{j} + a\sin\theta\,\mathbf{k} \qquad [52]$$

(see Figure 2). If μ_y and μ_z change slowly, the integrand decreases rapidly as $|x' - x_i'|$ increases. This condition is satisfied for slender bodies when the wavelength is large compared with the diameter of the body. We let

$$\mu_y(x_i') = \mu_y(x') + (x_i' - x')\frac{d\mu_y(x')}{dx'}$$

and [53]

$$\mu_z(x_i') = \mu_z(x') + (x_i' - x')\frac{d\mu_z(x')}{\partial x'}$$

We further assume that the contribution of the integrand to the value of the integral in Equation [51] is negligible except in the immediate neighborhood of x'. To the order of accuracy we are considering, we can then take the limits of integration as $(-\infty, +\infty)$ rather than $(-L/2, +L/2)$. Carrying out the integration, we obtain

$$\begin{aligned}\phi_S^* &= a(\mu_y\cos\theta + \mu_z\sin\theta)\int_{-\infty}^{+\infty}\frac{dx_i'}{R_i^3} \\ &= -a(v\cos\theta + w\sin\theta)\end{aligned} \qquad [54]$$

This should be quite accurate except at the ends of the body. We shall assume that the net effect of the error at the end of the body is of second order. Substituting in Equation [48] and integrating,

$$d\mathbf{M}_{t,s} = -\frac{2\pi^2}{\lambda}\rho a^2 x'(V\cos\beta - c)\left(\frac{u}{\cos\beta}\,\mathbf{j} + w\sin\beta\,\mathbf{k}\right)dx' \qquad [55]$$

If we combine Equations [43], [50], and [55], noting that on the path of integration $y' = 0$, we obtain

$$\begin{aligned}d\mathbf{M} = \rho A g h e^{-2\pi H/\lambda}\Bigg\{&\left[\frac{2\pi x'}{\lambda}\left(1 - \frac{V\cos\beta}{2c}\right)\sin\psi + \frac{V}{2c}\cos\psi\right]\mathbf{j} \\ &- \left[\frac{2\pi x'}{\lambda}\left(1 - \frac{V\cos\beta}{2c}\right)\cos\psi - \frac{V}{2c}\sin\psi\right]\sin\beta\,\mathbf{k}\Bigg\}dx'\end{aligned} \qquad [56]$$

The total pitching moment can then be written

$$M_y = \rho g h\, e^{-2\pi H/\lambda}\left[\frac{2\pi}{\lambda}\left(1-\frac{V\cos\beta}{2c}\right)\int_{-L/2}^{+L/2} Ax'\sin\psi\,dx' + \frac{V}{2c}\int_{-L/2}^{+L/2} A\cos\psi\,dx'\right] \quad [57]$$

and the total yawing moment

$$M_z = -\rho g h\, e^{-2\pi H/\lambda}\sin\beta\left[\frac{2\pi}{\lambda}\left(1-\frac{V\cos\beta}{2c}\right)\int_{-L/2}^{+L/2} Ax'\cos\psi\,dx' - \frac{V}{2c}\int_{-L/2}^{+L/2} A\sin\psi\,dx'\right] \quad [58]$$

INTEGRATION OF THE RESULTS

It is desirable to express the forces and moments in terms of dimensionless coefficients in order to be able to compare different bodies and different wave conditions. This will be done in the following way

$$C_f = \frac{F}{\rho g A_0 L}, \qquad C_m = \frac{M}{\rho g A_0{}^2}$$

where A_0 is the cross-sectional area at the midpoint of the axis of the body. While the dimensionless coefficients could be defined in other ways, some of which have definite advantages, the above forms have been adopted since they permit direct comparison of the effects of different wave systems upon a given body.

These coefficients can be given in a form which clearly shows their phase relationships to the wave train:

$$C_{f,x} = -\frac{\pi h}{2\lambda}\cos\beta\; e^{-2\pi H/\lambda}(b_0\cos\omega t - a_0\sin\omega t) \quad [59]$$

$$C_{f,y} = -\frac{\pi h}{\lambda}\sin\beta\left(1-\frac{V\cos\beta}{2c}\right)e^{-2\pi H/\lambda}(b_0\cos\omega t - a_0\sin\omega t) \quad [60]$$

$$C_{f,z} = -\frac{\pi h}{\lambda}\left(1-\frac{V\cos\beta}{2c}\right)e^{-2\pi H/\lambda}(a_0\cos\omega t + b_0\sin\omega t) \quad [61]$$

$$C_{m,y} = \frac{\pi h}{2\lambda}\,e^{-2\pi H/\lambda}\left\{\left[\left(1-\frac{V\cos\beta}{2c}\right)a_1 + \frac{\lambda}{\pi L}\,\frac{V}{2c}\,b_0\right]\cos\omega t + \left[\left(1-\frac{V\cos\beta}{2c}\right)b_1 - \frac{\lambda}{\pi L}\,\frac{V}{2c}\,a_0\right]\sin\omega t\right\} \quad [62]$$

$$C_{m,z} = -\frac{\pi h}{2\lambda} \sin\beta\, e^{-2\pi H/\lambda} \left\{ \left[\left(1 - \frac{V\cos\beta}{2c}\right) b_1 - \frac{\lambda}{\pi L}\,\frac{V}{2c}\, a_0 \right] \cos\omega t \right.$$

$$\left. - \left[\left(1 - \frac{V\cos\beta}{2c}\right) a_1 + \frac{\lambda}{\pi L}\,\frac{V}{2c}\, b_0 \right] \sin\omega t \right\} \qquad [63]$$

where ω is the frequency of encounter,

$$\omega = \frac{2\pi}{\lambda}\,(V\cos\beta - c) \qquad [64]$$

and

$$a_0 = \int_{-1}^{+1} \mathcal{A} \sin(\xi\gamma\cos\beta)\, d\xi \qquad [65]$$

$$a_1 = \int_{-1}^{+1} \mathcal{A}\,\xi \sin(\xi\gamma\cos\beta)\, d\xi \qquad [66]$$

$$b_0 = \int_{-1}^{+1} \mathcal{A} \cos(\xi\gamma\cos\beta)\, d\xi \qquad [67]$$

$$b_1 = \int_{-1}^{+1} \mathcal{A}\,\xi \cos(\xi\gamma\cos\beta)\, d\xi \qquad [68]$$

$$\mathcal{A} = \frac{A(\xi)}{A_0}, \quad \xi = \frac{2x'}{L} \qquad [69]$$

$$\gamma = \pi L/\lambda \qquad [70]$$

The coefficients a_0, a_1, b_0, b_1 depend only upon the form of the sectional-area curve and the ratio of the effective length of the body $L\cos\beta$ to the wavelength. Since most bodies which are of interest are nearly symmetric about the midsection, it is possible to obtain some idea of the relative magnitudes of these coefficients by observing that for symmetrical bodies, a_0 and b_1 vanish.

If the dimensionless sectional-area curve can be expressed as a polynomial, the integrations in Equations [65] to [68] can be carried out explicitly. For other functional forms, the coefficients will in general need to be evaluated by means of numerical quadratures. Since it is desirable to examine the variation of the force and moment coefficients with wavelength, these calculations could become lengthy and tedious. Therefore, it will usually be convenient to approximate the sectional-area curve by a polynomial, in order to take advantage of the explicit integrations.

One of the simplest procedures for approximating a function over a given range by a polynomial is to find the coefficients of the Fourier expansion in terms of Legendre polynomials. This method has the advantage that it yields the best least squares fit among all polynomials of any given degree. The coefficients are given by

$$c_i = \frac{2i+1}{2} \int_{-1}^{+1} \alpha(\xi)\, P_i(\xi)\, d\xi \qquad [71]$$

Then

$$\alpha(\xi) \doteq \sum_{i=0}^{n} c_i\, P_i(\xi) \qquad [72]$$

This procedure has the added advantage that the coefficients a_0, a_1, b_0, b_1 can be expressed directly in terms of the c_i's and the wavelength. We make use of the definite integrals (Reference 6, p. 50):

$$\int_{-1}^{+1} P_n(\xi)\cos x\xi\, d\xi = (-1)^{n/2}\, 2S_n(x) \quad \text{for } n \text{ even}$$

$$= 0 \quad \text{for } n \text{ odd}$$

$$\int_{-1}^{+1} P_n(\xi)\sin x\xi\, d\xi = 0 \quad \text{for } n \text{ even}$$

$$= (-1)^{\frac{n-1}{2}}\, 2S_n(x) \quad \text{for } n \text{ odd}$$

where $S_n(x) = \left(\frac{\pi}{2x}\right)^{1/2} J_{n+1/2}(x)$

The functions $S_n(x)$ are frequently called spherical Bessel functions. While for any value of n these functions can be written explicitly in formulas involving x and $\sin x$, it is more convenient to make use of extensive tables which exist for wide ranges of values of x and n.[7] We can write

$$a_0 = 2 \sum_{i=0}^{n} (-1)^i\, c_{2i+1}\, S_{2i+1}(\gamma \cos\beta) \qquad [73]$$

$$b_0 = 2 \sum_{i=0}^{n} (-1)^i\, c_{2i}\, S_{2i}(\gamma \cos\beta) \qquad [74]$$

Also, since

$$\xi P_n(\xi) = \frac{(n+1)\, P_{n+1} + n\, P_{n-1}}{2n+1}$$

We have

$$a_1 = \sum_{i=0}^{n} (-1)^{i+1}\, c_{2i}\, T_{2i}(\gamma \cos\beta) \qquad [75]$$

$$b_1 = \sum_{i=0}^{n} (-1)^i \, c_{2i+1} \, T_{2i+1}(\gamma \cos \beta) \qquad [76]$$

where

$$T_n(x) = \frac{2}{2n+1} [n \, S_{n-1}(x) - (n+1) \, S_{n+1}(x)]$$

The values of the coefficients have been computed for some sample bodies. These calculations, together with a recommended computational procedure, are described in Appendix 1. Also, in Appendix 2 a table is given for the spherical Bessel functions and for T_n for the n up to 6 and x up to 10. This is the range of greatest interest and practical importance.

DISCUSSION

The maximum values of the force and moment coefficients may be written

$$C_{f,x;\,\max} = \frac{\pi h}{2\lambda} \cos \beta \; e^{-2\pi H/\lambda} (a_0^2 + b_0^2)^{1/2} \qquad [77]$$

$$C_{f,y;\,\max} = 2 \, C_{f,x;\,\max} \left| \left(1 - \frac{V \cos \beta}{2c} \right) \tan \beta \right| \qquad [78]$$

$$C_{f,z;\,\max} = 2 \, C_{f,x;\,\max} \left| \frac{1 - \frac{V \cos \beta}{2c}}{\cos \beta} \right| \qquad [79]$$

$$C_{m,y;\,\max} = \frac{\pi h}{2\lambda} e^{-2\pi H/\lambda} \left[\left(1 - \frac{V \cos \beta}{2c} \right)^2 (a_1^2 + b_1^2) + \left(\frac{\lambda}{\pi L} \right)^2 \left(\frac{V}{2c} \right)^2 (a_0^2 + b_0^2) + 2 \left(1 - \frac{V \cos \beta}{2c} \right) \frac{\lambda}{\pi L} \frac{V}{2c} (a_1 b_0 - a_0 b_1) \right]^{1/2} \qquad [80]$$

$$C_{m,z;\,\max} = C_{m,y;\,\max} \, |\sin \beta| \qquad [81]$$

For the analysis of the effects on a body at a given depth and speed, more useful forms in terms of the Froude number $\mathcal{F}$ can be obtained:

$$C_{f,x;\,\max} = \frac{h \cos \beta}{\lambda} \, D \left(\frac{H}{L \cos \beta}, \gamma \cos \beta \right) \qquad [77a]$$

$$C_{f,y;\,\max} = \frac{2h}{\lambda} D\left(\frac{H}{L\cos\beta}, \gamma\cos\beta\right)\left|\left(1 - \mathcal{F}\cos^{1/2}\beta\sqrt{\frac{\gamma\cos\beta}{2}}\right)\sin\beta\right| \quad [78a]$$

$$C_{f,z;\,\max} = \frac{2h}{\lambda} D\left(\frac{H}{L\cos\beta}, \gamma\cos\beta\right)\left|1 - \mathcal{F}\cos^{1/2}\beta\sqrt{\frac{\gamma\cos\beta}{2}}\right| \quad [79a]$$

$$C_{m,y;\,\max} = \frac{h}{\lambda} e^{-2\left(\frac{H}{L\cos\beta}\right)\gamma\cos\beta} G(\mathcal{F}\cos^{1/2}\beta, \gamma\cos\beta) \quad [80a]$$

$$C_{m,z;\,\max} = \frac{h}{\lambda} e^{-2\left(\frac{H}{L\cos\beta}\right)\gamma\cos\beta} |\sin\beta| G(\mathcal{F}\cos^{1/2}\beta, \gamma\cos\beta) \quad [81a]$$

where

$$\mathcal{F} = \frac{V}{\sqrt{gL}}$$

$$D\left(\frac{H}{L\cos\beta}, \gamma\cos\beta\right) = \frac{\pi}{2} e^{-2\left(\frac{H}{L\cos\beta}\right)\gamma\cos\beta} (a_0^2 + b_0^2)^{1/2}$$
$$= \frac{\pi}{2} e^{-2\left(\frac{H}{L\cos\beta}\right)\gamma\cos\beta}\left|\frac{b_0}{\cos\epsilon_1}\right| \quad [82]$$

$$G(\mathcal{F}\cos^{1/2}\beta, \gamma\cos\beta) = \frac{\pi}{2}\left[\left(1 - \mathcal{F}\cos\beta\sqrt{\frac{\gamma}{2}}\right)^2 (a_1^2 + b_1^2) + \frac{\mathcal{F}^2}{2\gamma}(a_0^2 + b_0^2)\right.$$
$$\left. + \mathcal{F}\sqrt{\frac{2}{\gamma}}\left(1 - \mathcal{F}\cos\beta\sqrt{\frac{\gamma}{2}}\right)(a_1 b_0 - a_0 b_1)\right]^{1/2} \quad [83]$$
$$= \frac{\pi}{2|\cos\epsilon_2|}\left|\left(1 - \mathcal{F}\cos^{1/2}\beta\sqrt{\frac{\gamma\cos\beta}{2}}\right)a_1 + \frac{b_0\mathcal{F}\cos^{1/2}\beta}{\sqrt{2\gamma\cos\beta}}\right|$$

$$\tan\epsilon_1 = \frac{a_0}{b_0} \quad [84]$$

$$\tan \epsilon_2 = \frac{\left(1 - \frac{V \cos \beta}{2c}\right) b_1 - \frac{\lambda}{\pi L} \frac{V}{2c} a_0}{\left(1 - \frac{V \cos \beta}{2c}\right) a_1 + \frac{\lambda}{\pi L} \frac{V}{2c} b_0} \qquad [85]$$

$$= \frac{\left(1 - \mathcal{F} \cos^{1/2} \beta \sqrt{\frac{\gamma \cos \beta}{2}}\right) b_1 - \left(a_0 \mathcal{F} \cos^{1/2} \beta\right) \sqrt{2\gamma \cos \beta}}{\left(1 - \mathcal{F} \cos^{1/2} \beta \sqrt{\frac{\gamma \cos \beta}{2}}\right) a_1 + \left(b_0 \mathcal{F} \cos^{1/2} \beta\right) \sqrt{2\gamma \cos \beta}}$$

It may be seen that the ratios of the heaving and swaying forces to the axial, or surging, force depend only upon $\mathcal{F}$, γ, and β, and are independent of the form of the body. The quantity $\mathcal{F} \cos^{1/2} \beta$, which appears in the above formulas, can be written $(V \cos \beta)/\sqrt{gL \cos \beta}$ and is thus the Froude number for the motion relative to a line perpendicular to the wave crests.

The phase relations of the forces and moments to the wave train depend upon the angles ϵ_1 and ϵ_2 defined above. These relationships are exhibited in the phase diagrams, Figures 4a and 4b. These may be summarized as follows:

F_x follows η by $\frac{\pi}{2} - \epsilon_1$

M_y leads η by $\frac{\pi}{2} - \epsilon_2$

M_z follows η by ϵ_2

and for $V \cos \beta < 2c$

F_y follows η by $\frac{\pi}{2} - \epsilon_1$

F_z follows η by $\pi - \epsilon_1$

while for $V \cos \beta > 2c$

F_y leads η by $\frac{\pi}{2} + \epsilon_1$

F_z leads η by ϵ_1

In the particular case in which the body is symmetrical fore and aft, the coefficients a_0 and b_1 are zero, and the phase angles become

$$\epsilon_1 = 0 \quad \text{for} \quad b_0 > 0$$
$$= 180° \quad \text{for} \quad b_0 < 0 \qquad [84a]$$

$$\epsilon_2 = 0 \quad \text{for denominator of [85]} > 0$$
$$= 180° \quad \text{for denominator of [85]} < 0 \qquad [85a]$$

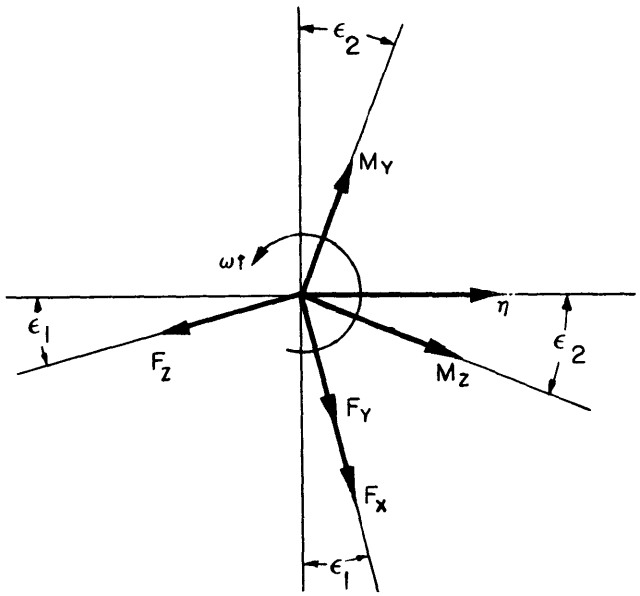

Figure 4a - $V \cos\beta < 2c$

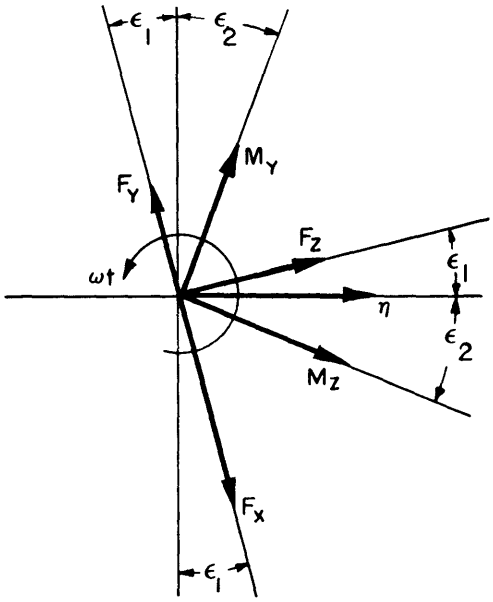

Figure 4b - $V \cos \beta > 2c$

Figure 4 - Phase Diagrams

Since in this case $|\cos \epsilon_1| = |\cos \epsilon_2| = 1$ the formulas for D and G are also slightly simplified.

From an examination of the formulas presented in this and the previous section, several important relationships predicted by the slender body theory can be observed:

1. The forces and moments are directly proportional to the area of the midship section, and hence to the square of the diameter. This relation will certainly break down for small fineness ratios. An indication of the range of validity of this result, and therefore of this entire investigation, will be available from the forthcoming studies of the spheroid.

2. For waves of a given length, the forces and moments are directly proportional to the wave height h.

3. The forces and moments decrease exponentially with depth of submergence, the rate of decrease depending upon γ and, therefore, upon the ratio of the wavelength to the body length. The greater this ratio, the smaller the rate of decrease. Only waves of length greater than three times the depth are likely to be of significance.

4. The maximum value of the oscillating axial force, or surging force, is independent of the forward velocity of the body, but the moments and the transverse forces are linear functions of the ratio of velocity of the body to the celerity of the waves. In particular, when $V \cos \beta = 2c$, the vertical and side forces are identically zero.

5. The ratios of the maximum vertical and side forces to the maximum surging force are independent of the form of the body and are uniquely determined when $\mathcal{F}$, γ, and β are given.

6. The phase relations between the forces and the wave train are independent of the forward velocity, except for a phase reversal for F_y and F_z at $V \cos \beta = 2c$. For bodies symmetrical fore and aft, all phase differences are multiples of $\pi/2$.

7. While it is not evident from the equations, the sample computations given in Appendix 1 indicate that for bodies of "reasonable" form, wavelengths less than half the body length are likely to have negligible effects.

CONCLUSION

We have found values for the forces and moments acting on a body of revolution moving beneath a regular wave train under the following assumptions:

1. The fluid is non-viscous, and the flow is irrotational.

2. The free surface satisfies the linearized boundary condition.

3. The wavelength and the length of the body are both large compared with the maximum diameter of the body.

The forces and moments have been expressed in relatively simple formulas depending upon the Froude number, the ratio of the wavelength to the body length, the height-length ratio of the wave, the ratio of the depth of submergence to the length of the body, and the shape of the sectional-area curve. A procedure has been given for computing these forces and moments for any given body of revolution when the sectional-area curve is given.

ACKNOWLEDGMENT

Most of the computations in this report were carried out by Mrs. Alice Thorpe, who was also very helpful in checking the algebraic operations.

APPENDIX 1 - NUMERICAL EXAMPLES

In this appendix, the force and moment coefficients will be found for three sample bodies, and a recommended procedure will be described for carrying out the computations for an arbitrary body of revolution.

Example 1

For the first example, we consider the spheroid, which has the dimensionless sectional area curve:

$$\mathcal{A}(\xi) = 1 - \xi^2 = \frac{2}{3}\left[P_0(\xi) - P_2(\xi)\right]$$

(A list of the first seven Legendre polynomials is given in Appendix 2.) This expression for $\mathcal{A}(\xi)$ is in the form of Equation [71] with

$$c_0 = \frac{2}{3}, \quad c_1 = 0, \quad c_2 = -\frac{2}{3}$$

The function $\mathcal{A}(\xi)$ as well as the dimensionless profile are shown in Figure 5. Since the body is symmetrical about $\xi = 0$, we have

$$a_0 = b_1 = 0$$

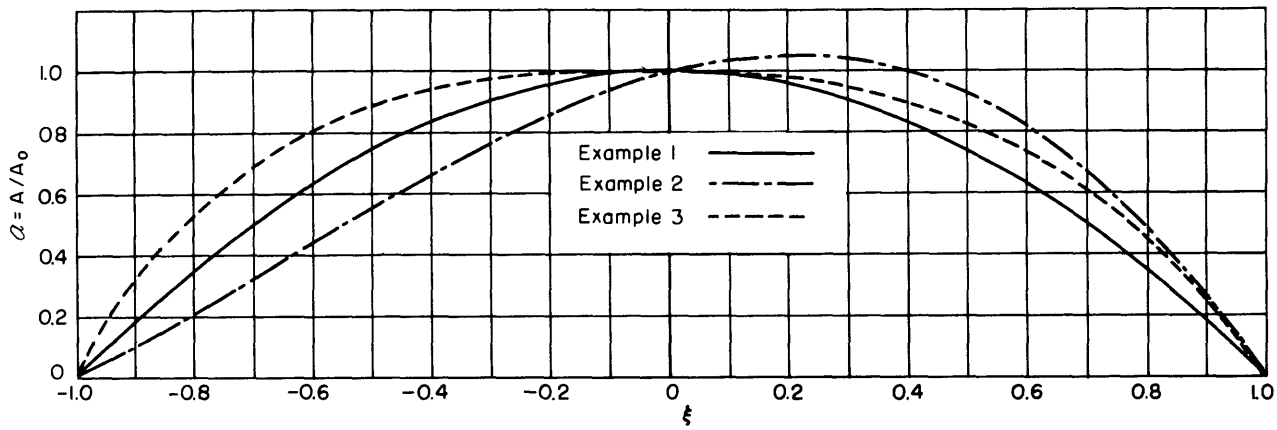

Figure 5a - Sectional-Area Curves

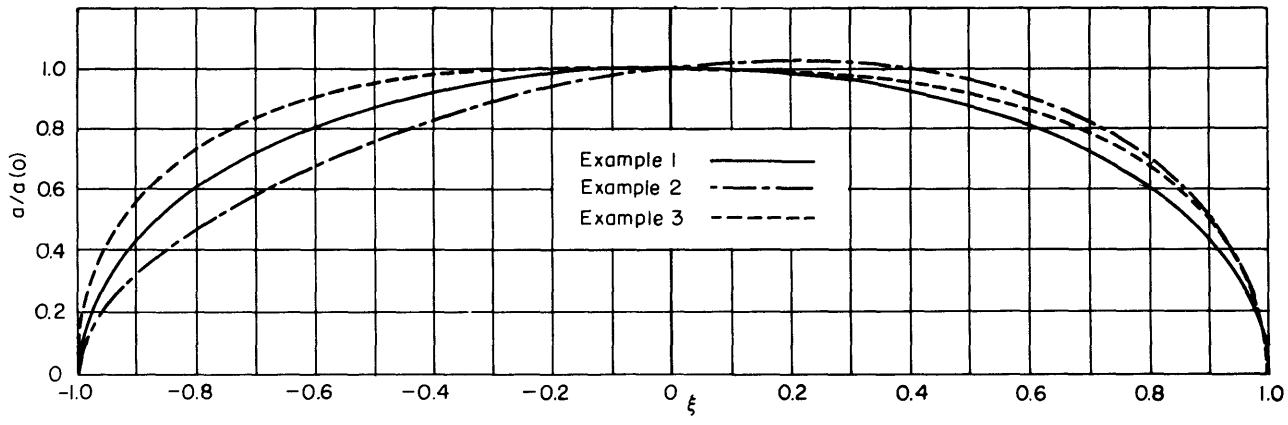

Figure 5b - Profiles

Figure 5 - Sectional-Area and Profile Curves for Three Sample Bodies

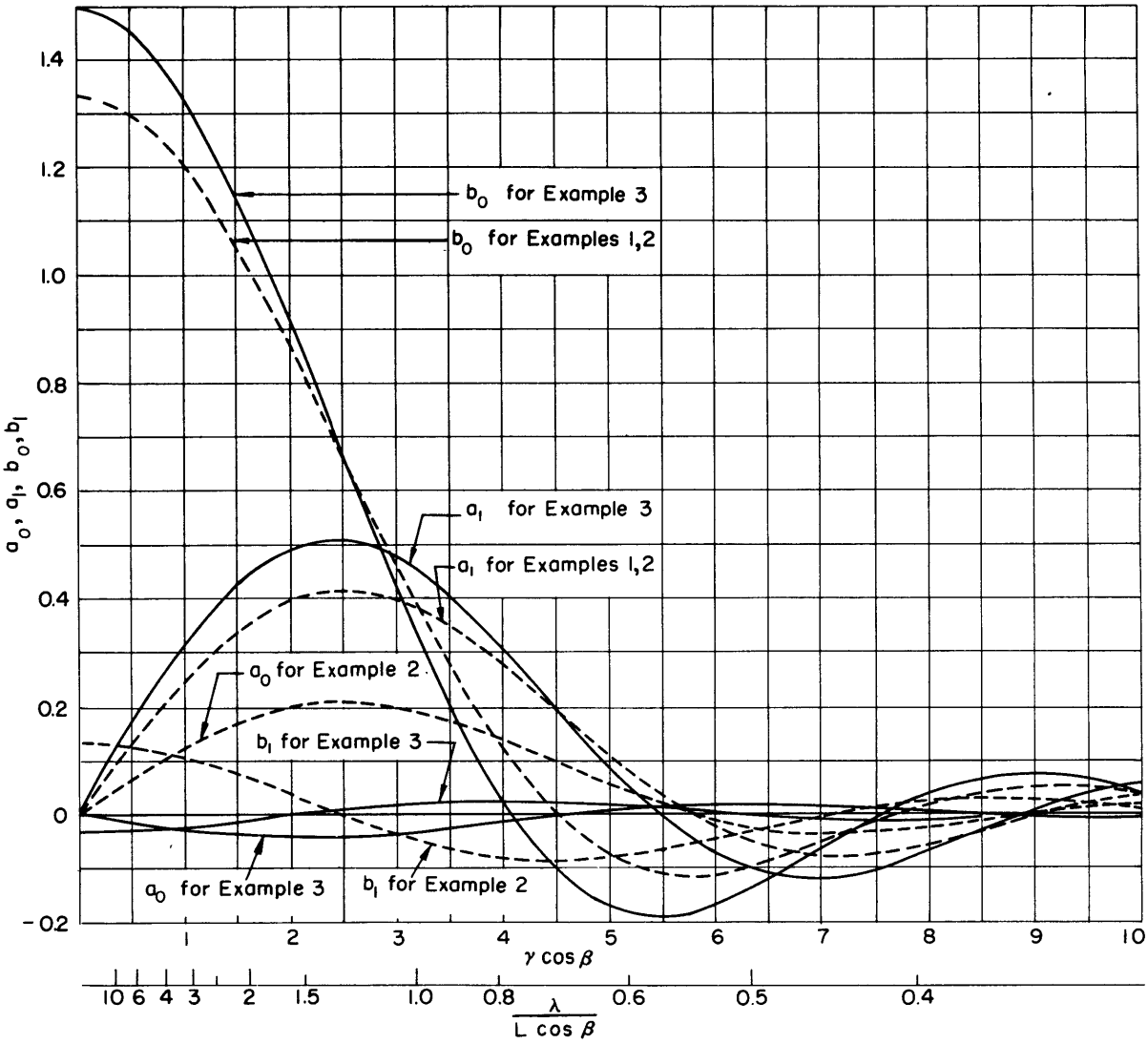

Figure 6 - a_0, a_1, b_0, b_1 for Sample Bodies

From Equations [75] and [74], the other coefficients are

$$a_1 = -\frac{2}{3}\left[T_0(\gamma \cos \beta) + T_2(\gamma \cos \beta)\right]$$

$$b_0 = \frac{4}{3}\left[S_0(\gamma \cos \beta) + S_2(\gamma \cos \beta)\right]$$

These coefficients are plotted in Figure 6 as functions of $\gamma \cos \beta$, with an indication of the corresponding values of $\lambda/L \cos \beta$. The angles ϵ_1 and ϵ_2 are identically zero or 180 degrees, because of symmetry. The functions $D[H/(L \cos \beta), \gamma \cos \beta]$ and $G(\mathcal{F}\cos^{1/2}\beta, \gamma \cos \beta)$ can then be computed from Equations [82] and [83]. These are plotted in Figures 7 and 8. The values of the maximum lifting force and pitching moment coefficients are plotted for certain values of the various parameters in Figure 9.

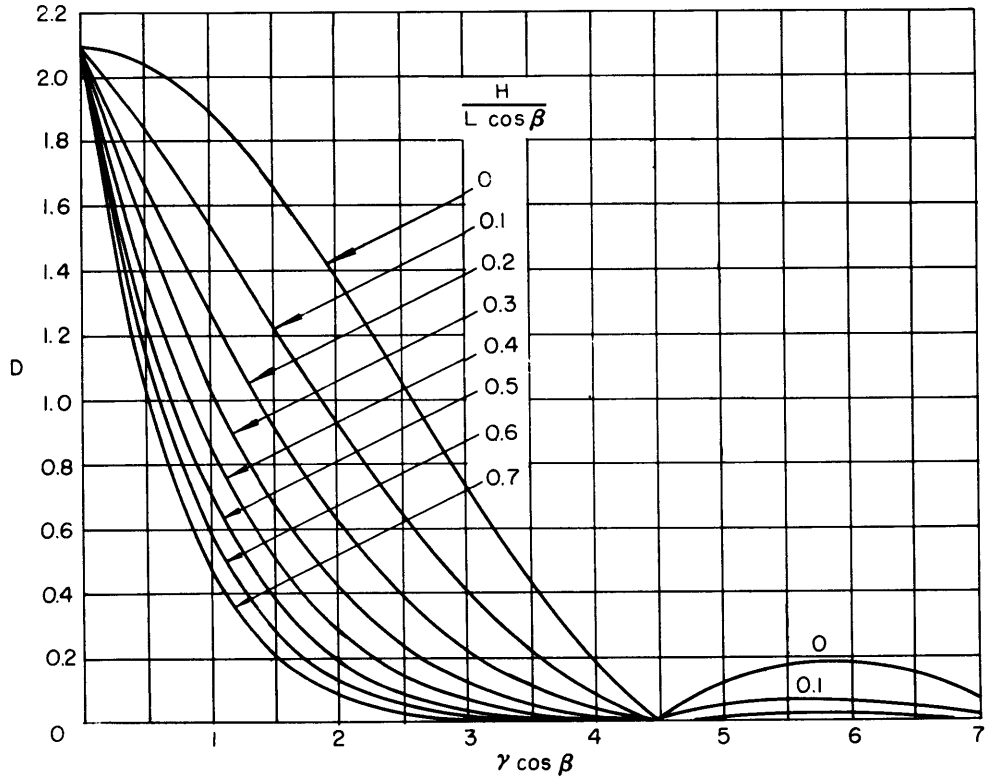

Figure 7 - $D[H/(L \cos \beta), \gamma \cos \beta]$ for Example 1

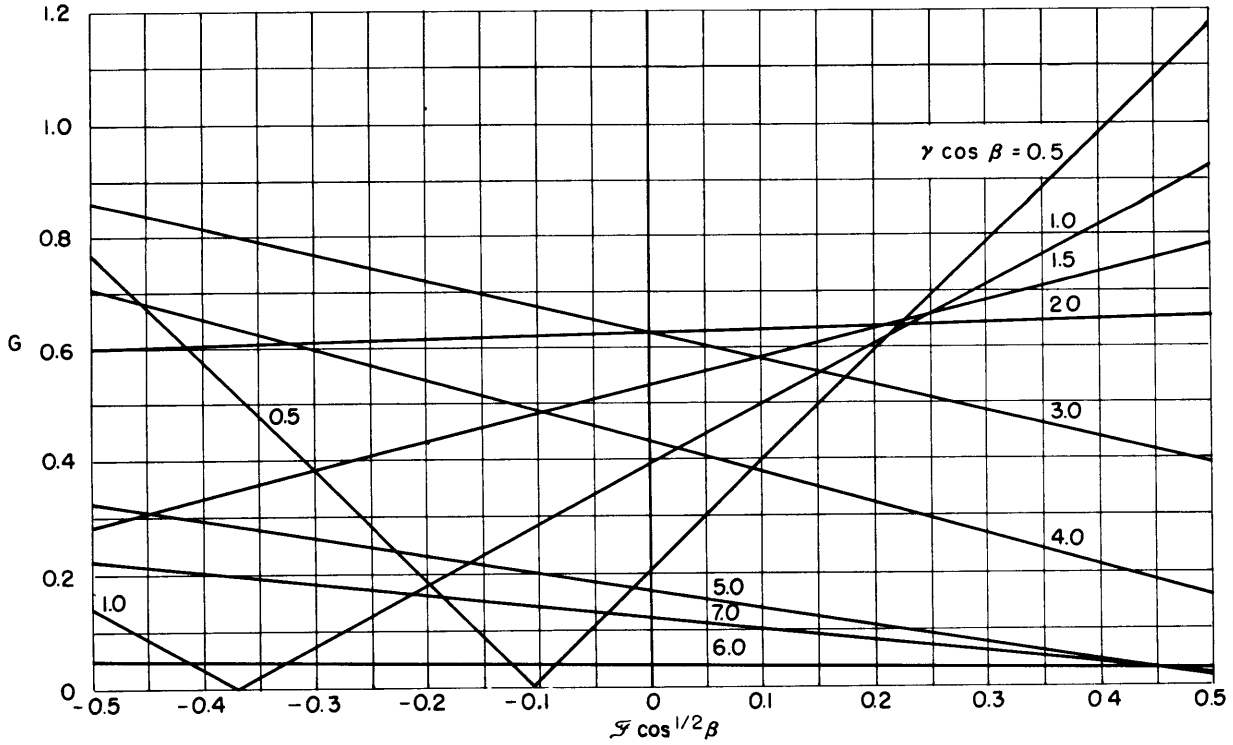

Figure 8 - $G(\mathcal{F} \cos^{1/2} \beta, \gamma \cos \beta)$ for Example 1

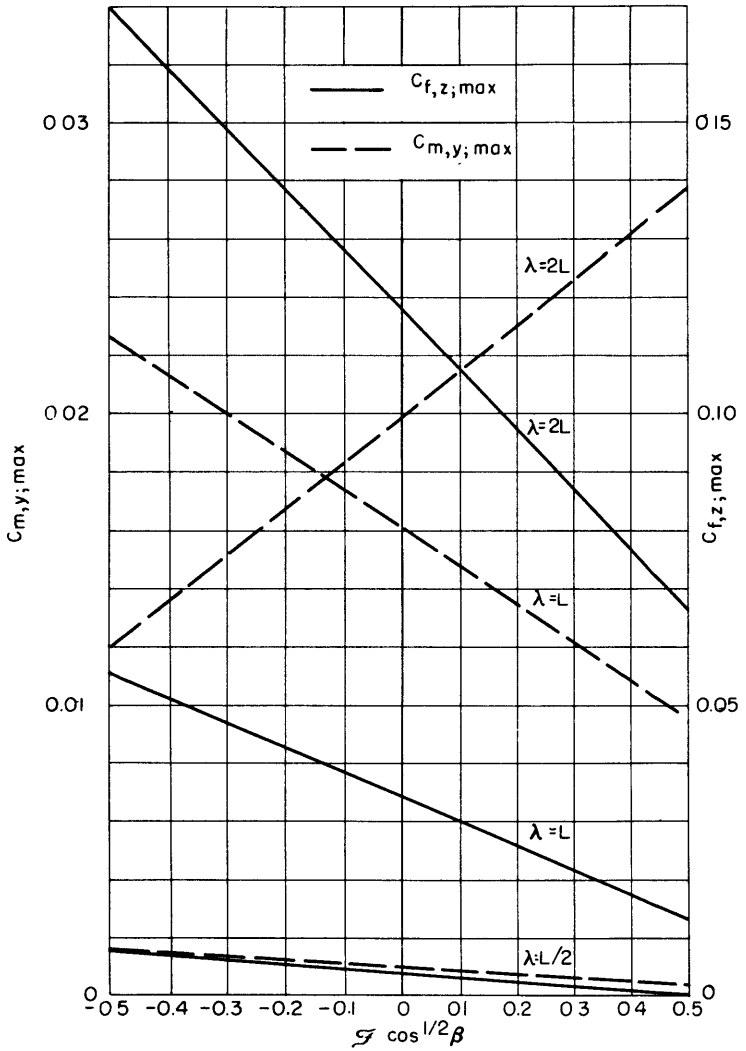

Figure 9a - $H/(L\cos\beta) = 0.1$

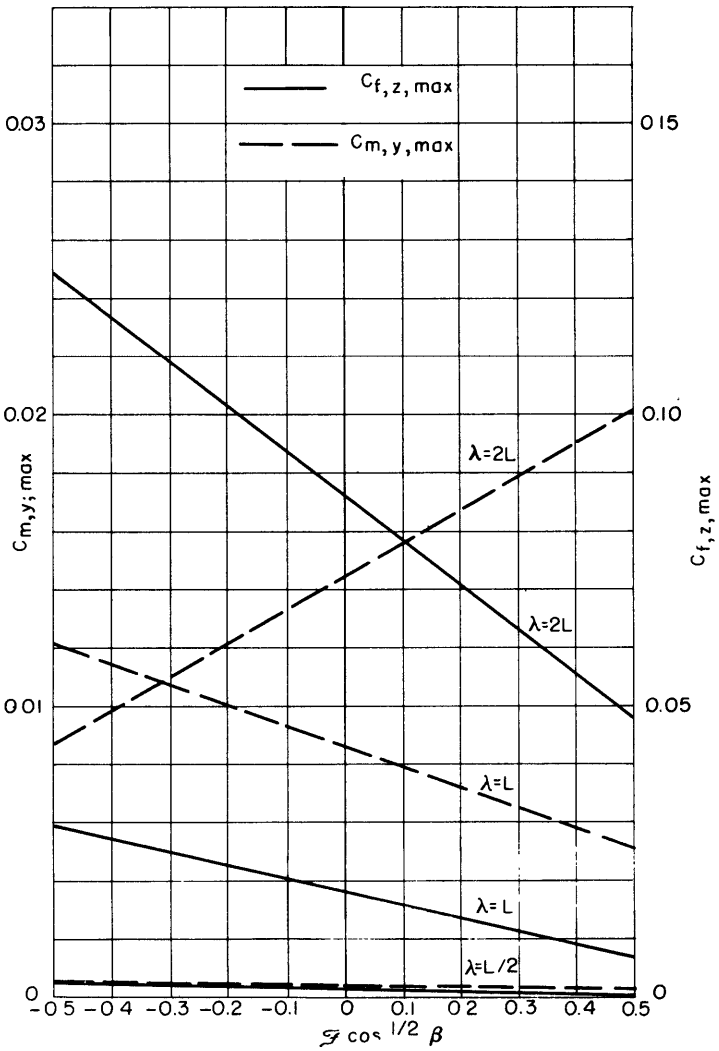

Figure 9b - $H/(L\cos\beta) = 0.2$

Figure 9 - Lifting Force and Pitching Moment Coefficients for Example 1 for $h/\lambda = 1/20$

Example 2

For our second example, we modify the sectional-area curve for the spheroid by adding a skew-symmetric portion:

$$\mathcal{A}(\xi) = 1 - \xi^2 + \frac{1}{2}\xi(1 - \xi^2)$$

$$= \frac{2}{3}P_0(\xi) + \frac{1}{5}P_1(\xi) - \frac{2}{3}P_2(\xi) - \frac{1}{5}P_3(\xi)$$

The profile and sectional-area curve are shown in Figure 5. The values of a_1 and b_0 remain unchanged, but a_0 and b_1 are no longer zero.

$$a_0 = \frac{2}{5}[S_1(\gamma \cos \beta) + S_3(\gamma \cos \beta)]$$

$$a_1 = -\frac{2}{3}[T_0(\gamma \cos \beta) + T_2(\gamma \cos \beta)]$$

$$b_0 = \frac{4}{3}[S_0(\gamma \cos \beta) + S_2(\gamma \cos \beta)]$$

$$b_1 = \frac{1}{5}[T_1(\gamma \cos \beta) + T_3(\gamma \cos \beta)]$$

These are shown in Figure 6. The angles ϵ_1 and ϵ_2 are computed, using Equations [84] and [85]. Plots are shown in Figures 10 and 11. D and G are shown in Figures 12 and 13. Certain values of $C_{f,z;\max}$ and $C_{m,y;\max}$ are given in Figure 14.

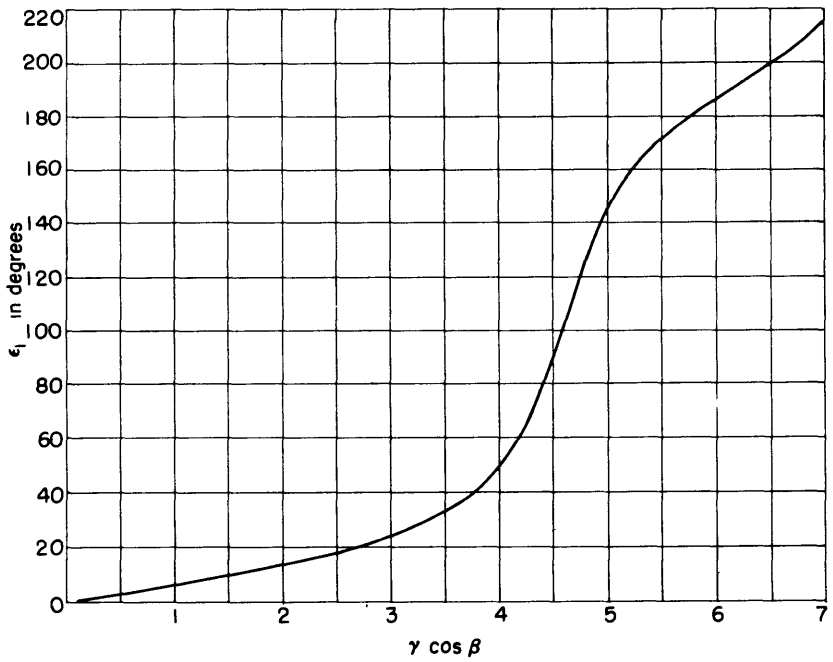

Figure 10 - $\epsilon_1(\gamma \cos \beta)$ for Example 2

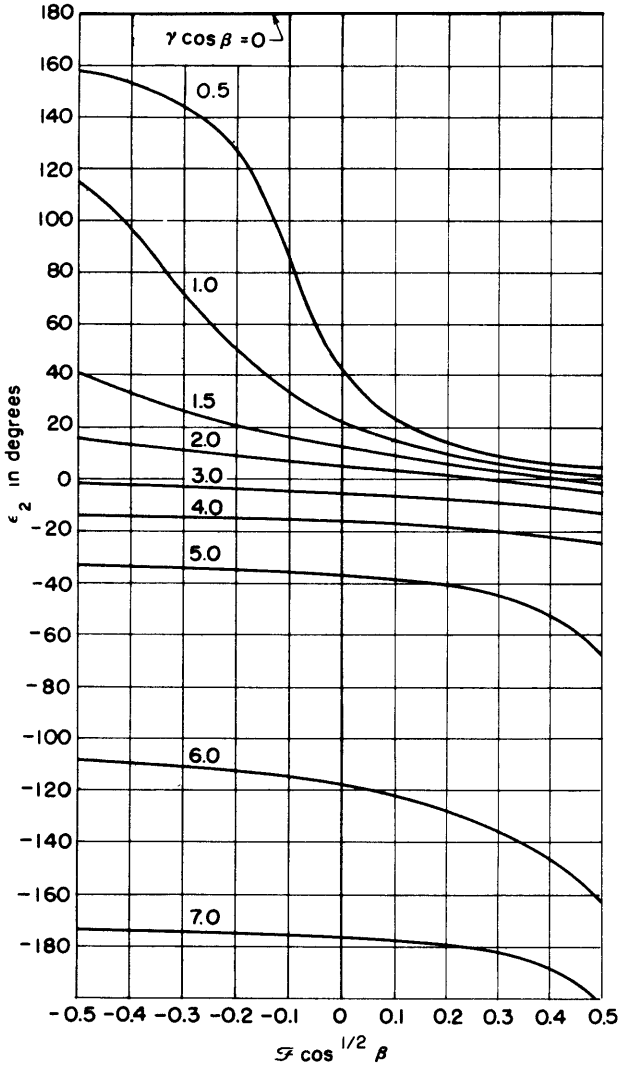

Figure 11 - $\epsilon_2(\mathcal{F}\cos^{1/2}\beta, \gamma\cos\beta)$ for Example 2

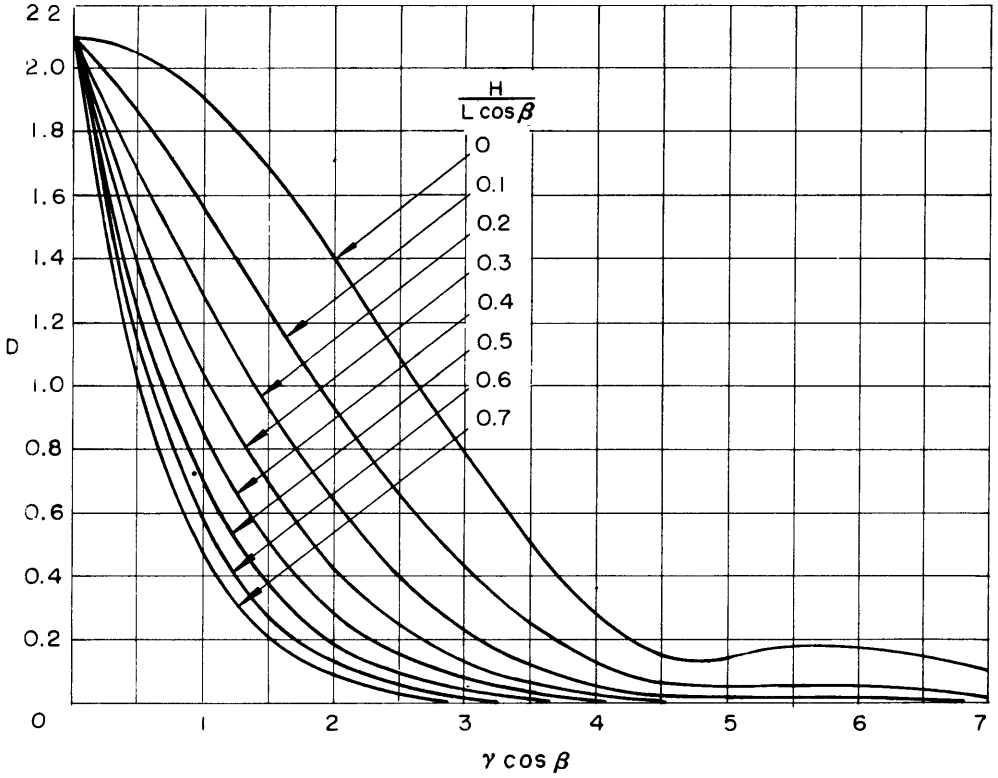

Figure 12 - $D(H/L\cos\beta), \gamma\cos\beta)$ for Example 2

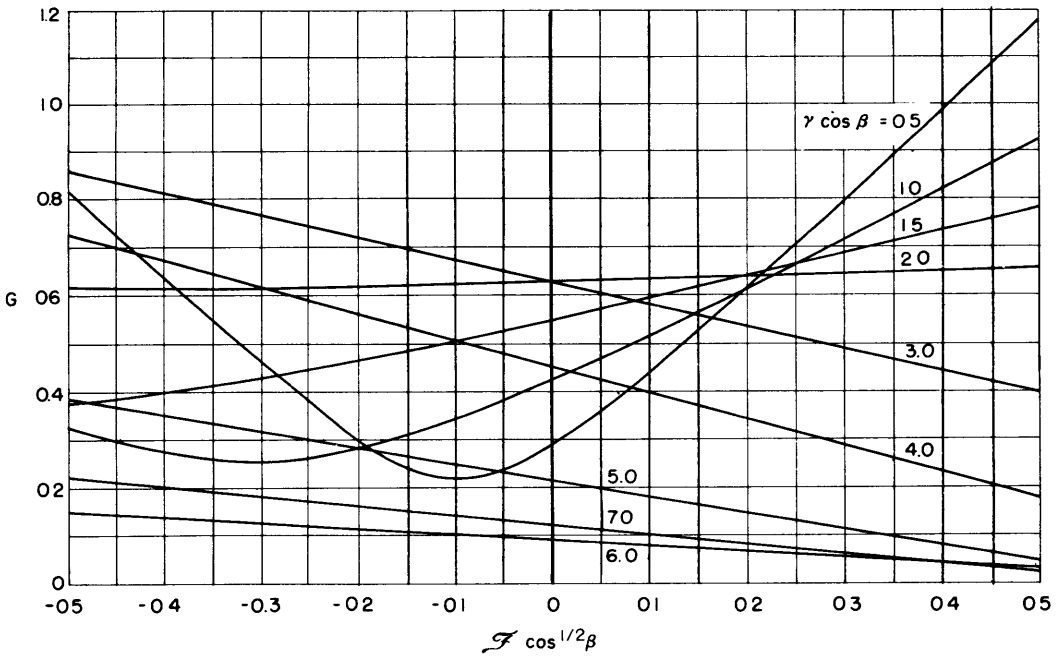

Figure 13 - $G(\mathcal{F}\cos^{1/2}\beta, \gamma\cos\beta)$ for Example 2

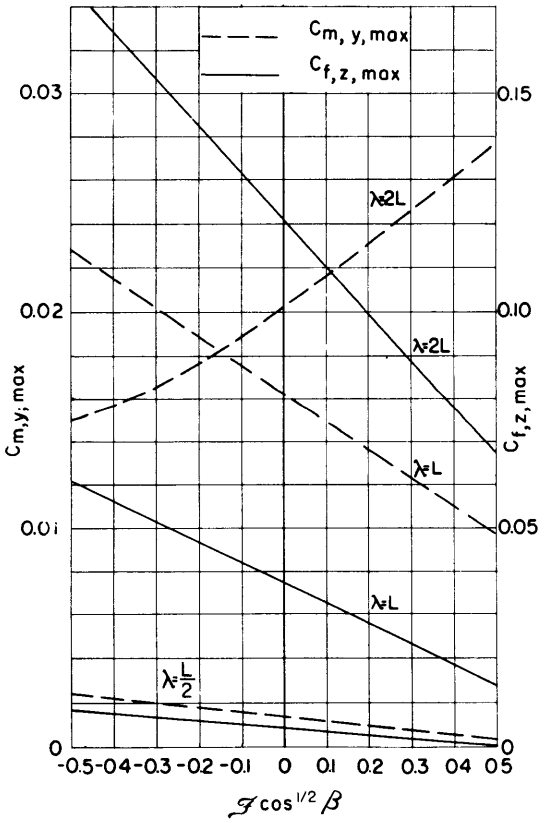

Figure 14a - $H/L\cos\beta = 0.1$

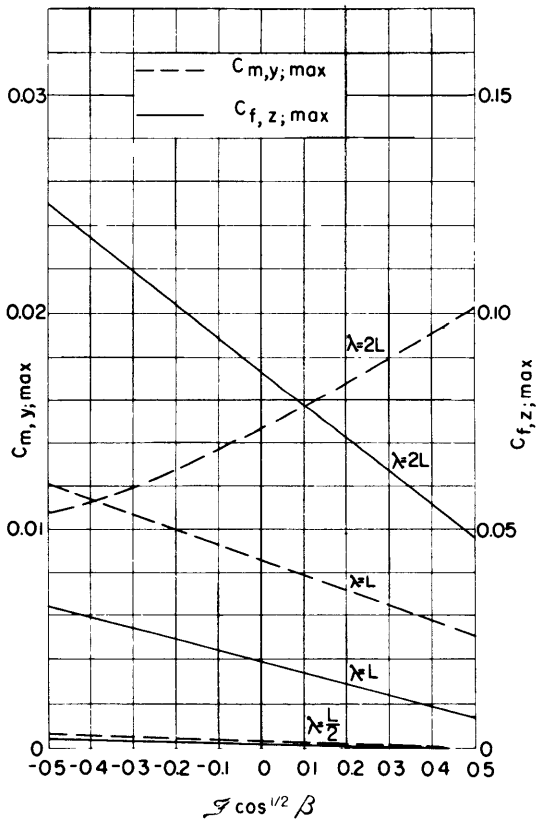

Figure 14b - $H/L\cos\beta = 0.2$

Figure 14 - Lifting Force and Pitching Moment Coefficients for Example 2 for $h/\lambda = 1/20$

Example 3 - Arbitrary body

For our final example we consider the body of revolution with the dimensionless sectional-area curve shown in Figure 5a.

We must first evaluate the coefficients $\{c_i\}$ in Equation [72]. An analytic expression for $a(\xi)$ is not available, and it is necessary that the quadratures in Equation [71] be carried out numerically. This could be done by Simpson's rule or any other standard procedure, but a very convenient procedure can be based on the Gauss mechanical quadrature formula.[8] Table 4 in Appendix 2 is derived from this formula and can be used to obtain the $\{c_i\}$ directly by means of the relation

$$c_i = \sum_{j=0}^{6} a(\xi_j)\, d_{ij}$$

The values for this body of revolution are

$c_0 = 0.6711$ $\quad c_1 = 0.0754$ $\quad c_2 = 0.6817$ $\quad c_3 = 0.0228$

$c_4 = 0.0012$ $\quad c_5 = 0.0654$ $\quad c_6 = 0.0400$

Once the $\{c_i\}$ are obtained, the procedure is identical with that in the previous examples. The results of the computation are shown in Figures 6, 15, 16, 17, 18, and 19.

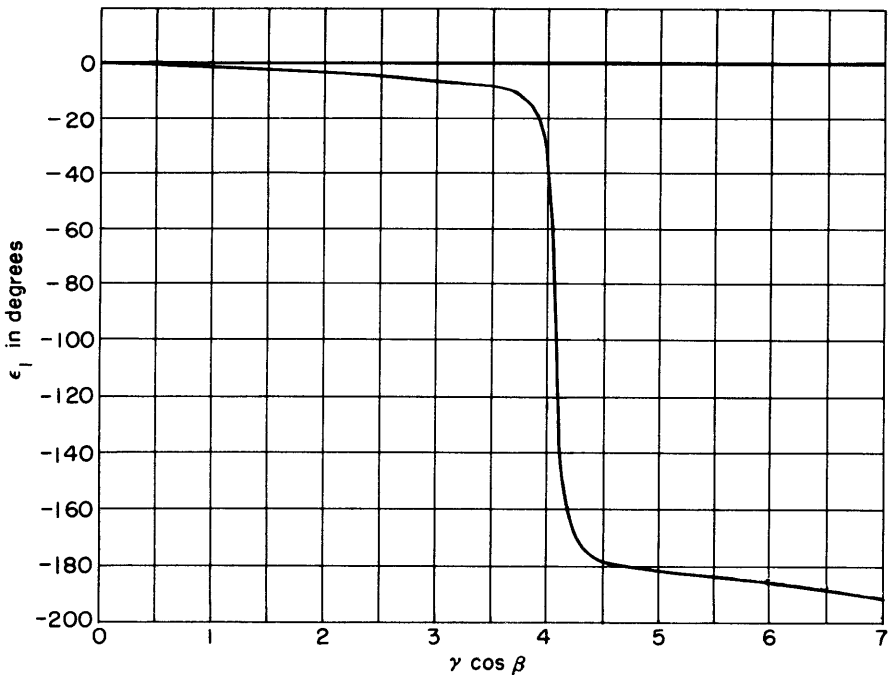

Figure 15 - $\epsilon_1(\gamma \cos \beta)$ for Example 3

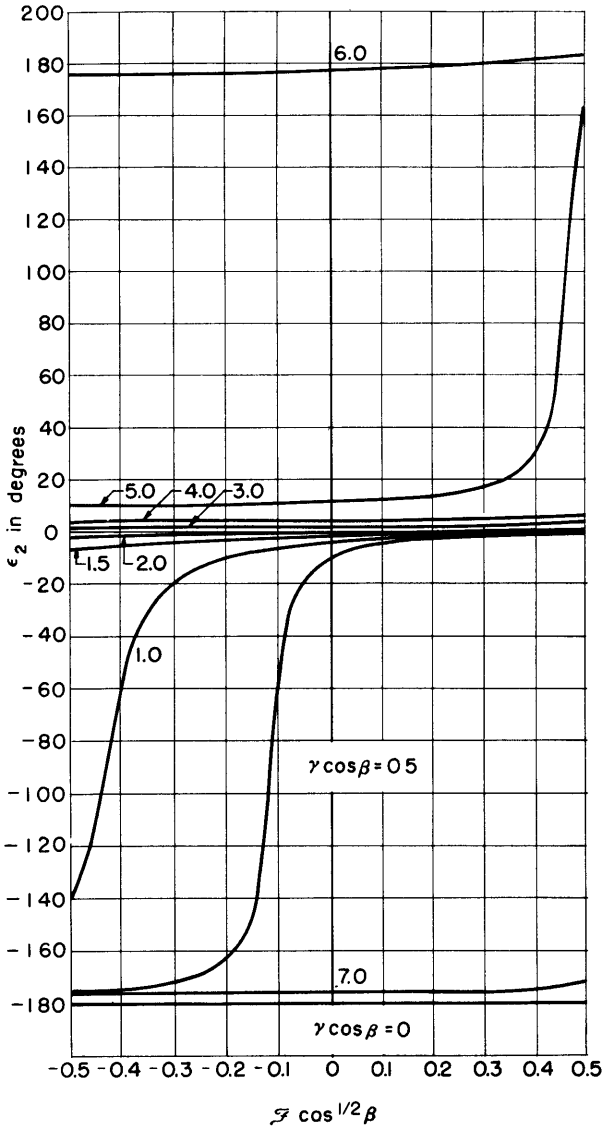

Figure 16 - $\epsilon_2(\mathcal{F}\cos^{1/2}\beta, \gamma\cos\beta)$ for Example 3

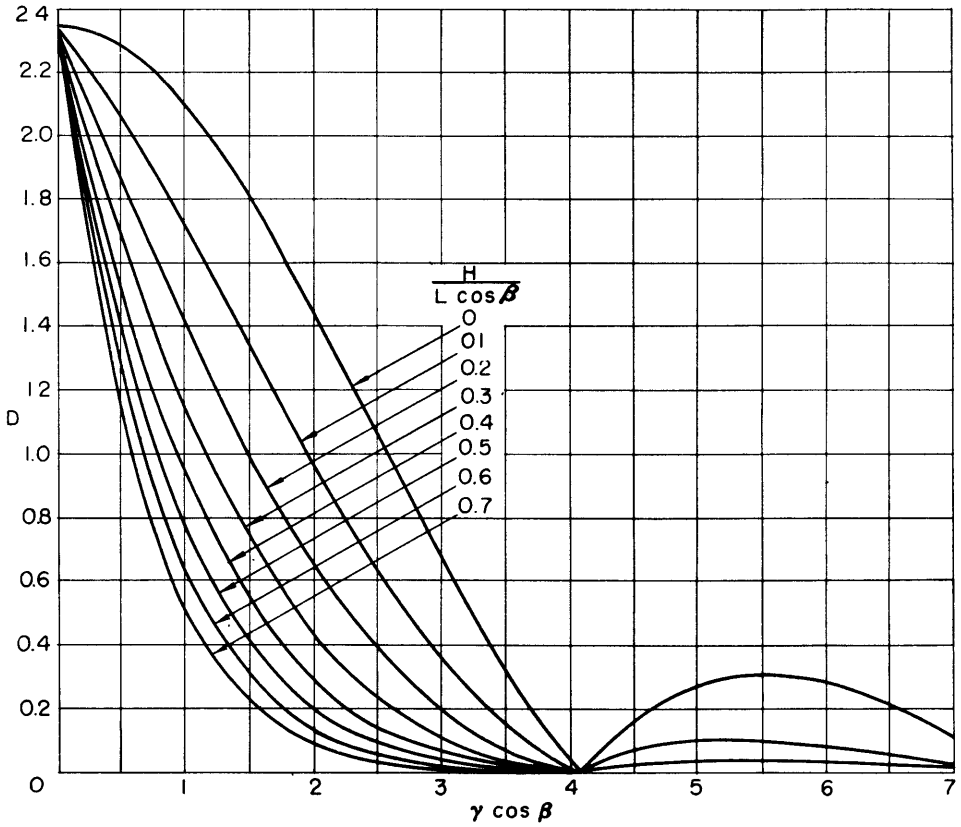

Figure 17 - $D[H/(L\cos\beta), \gamma\cos\beta]$ for Example 3

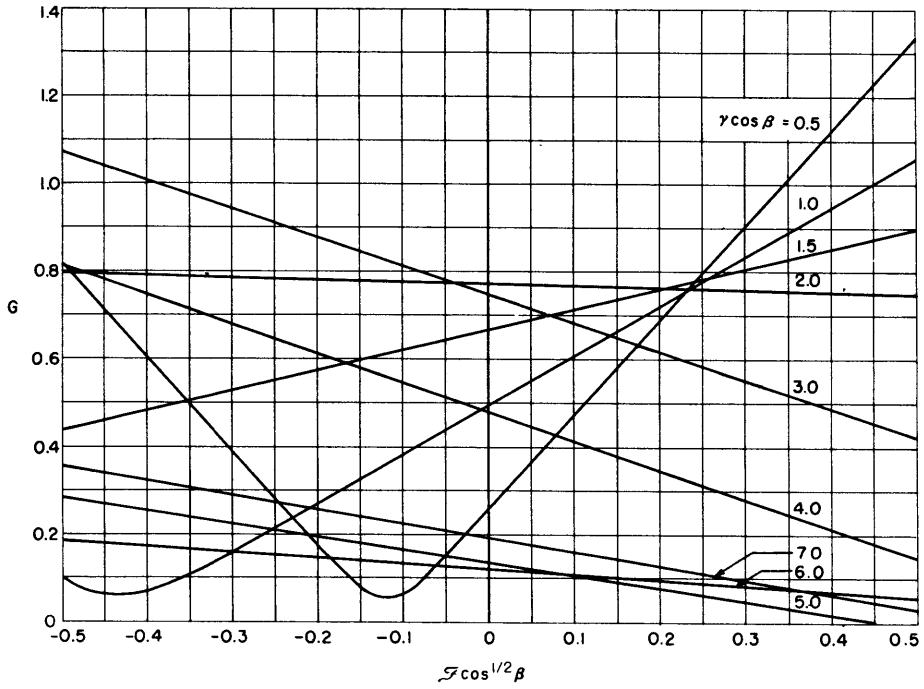

Figure 18 - $G(\mathcal{F}\cos^{1/2}\beta, \gamma\cos\beta)$ for Example 3

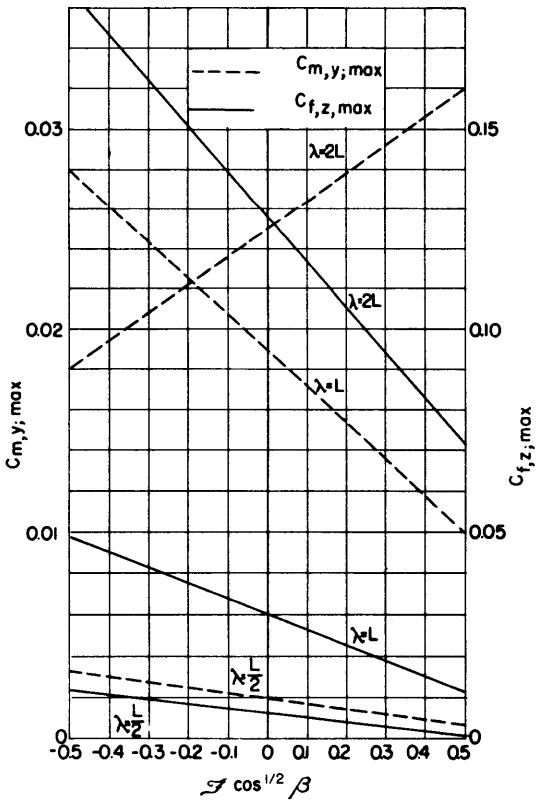

Figure 19a $H/L\cos\beta = 0.1$

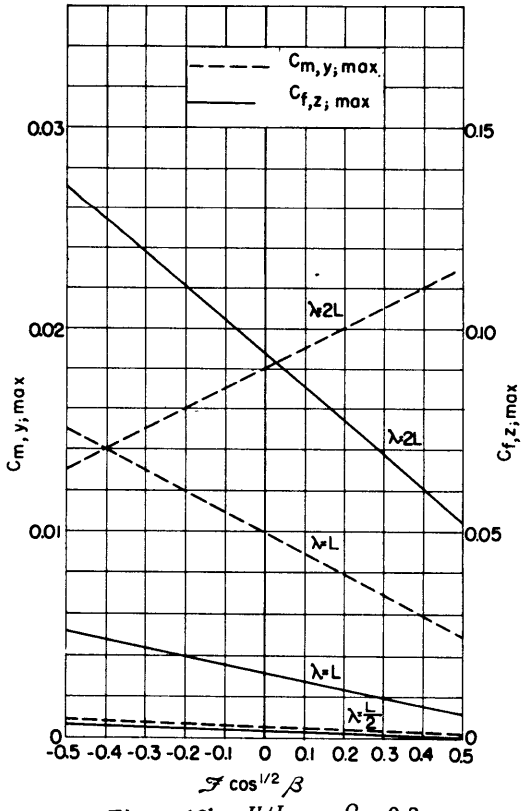

Figure 19b - $H/L\cos\beta = 0.2$

Figure 19 - Lifting Force and Pitching Moment Coefficients for Example 3 for $h/\lambda = 1/20$

DISCUSSION OF EXAMPLES

There are significant differences between the sectional area curves for the three examples which have been computed. Nevertheless, the similarities between the results for the different bodies are more conspicuous than their differences. In particular:

1. The over-all pattern of the results is preserved. This is shown by a comparison of Figures 7, 12, 17, and Figures 8, 13, 18.

2. The effect of the rather high degree of asymmetry in Example 2 is evident in a rounding of the cusps in the D and G curves, but it is otherwise barely noticeable.

3. The fuller form of Example 3, as compared to Example 1, results in appreciable changes in magnitude in the D and G functions, but again, the over-all patterns are very similar.

4. Figures 8, 13, and 18 show that except near a "cusp," the function G is virtually a linear function of the Froude number for a fixed $\gamma \cos \beta$. Hence, the amplitude of the moment is very nearly a linear function of the Froude number for a given wavelength.

5. In all three cases the effects are quite small for wavelengths less than half the body length ($\gamma > 2\pi$). This supports the statement made previously that for such waves the effects are negligible.

APPENDIX 2

TABLES

TABLE 1

The Legendre Polynomials

$$P_0 = 1$$

$$P_1 = x$$

$$P_2 = \frac{1}{2}(3x^2 - 1)$$

$$P_3 = \frac{1}{2}(5x^3 - 3x)$$

$$P_4 = \frac{1}{8}(35x^4 - 30x^2 + 3)$$

$$P_5 = \frac{1}{8}(63x^5 - 70x^3 + 15x)$$

$$P_6 = 16(231x^6 - 315x^4 + 105x^2 - 5)$$

TABLE 2

$$S_n(x) = \left(\frac{\pi}{2x}\right)^{1/2} J_{n+1/2}(x)$$

x	$S_0(x)$	$S_1(x)$	$S_2(x)$	$S_3(x)$	$S_4(x)$	$S_5(x)$	$S_6(x)$
0.0	+1.0000	0.0000	0.0000	0.0000	0.0000	0.0000	0.0000
0.5	+0.9589	+0.1625	+0.0164	+0.0012	+0.0001	+0.0000	+0.0000
1.0	+0.8415	+0.3012	+0.0620	+0.0090	+0.0010	+0.0001	+0.0000
1.5	+0.6650	+0.3962	+0.1273	+0.0283	+0.0048	+0.0007	+0.0001
2.0	+0.4546	+0.4354	+0.1984	+0.0607	+0.0141	+0.0026	+0.0004
2.5	+0.2394	+0.4162	+0.2601	+0.1039	+0.0309	+0.0074	+0.0015
3.0	+0.0470	+0.3457	+0.2986	+0.1521	+0.0561	+0.0164	+0.0040
3.5	−0.1002	+0.2389	+0.3050	+0.1968	+0.0886	+0.0310	+0.0089
4.0	−0.1892	+0.1161	+0.2763	+0.2292	+0.1249	+0.0518	+0.0175
4.5	−0.2172	−0.0014	+0.2163	+0.2417	+0.1598	+0.0778	+0.0304
5.0	−0.1918	−0.0951	+0.1347	+0.2298	+0.1870	+0.1068	+0.0480
5.5	−0.1283	−0.1522	+0.0453	+0.1933	+0.2008	+0.1352	+0.0697
6.0	−0.0466	−0.1678	−0.0373	+0.1367	+0.1968	+0.1585	+0.0938
6.5	+0.0331	−0.1452	−0.1001	+0.0682	+0.1735	+0.1721	+0.1177
7.0	+0.0939	−0.0943	−0.1343	−0.0016	+0.1327	+0.1722	+0.1379
7.5	+0.1251	−0.0295	−0.1369	−0.0617	+0.0793	+0.1569	+0.1508
8.0	+0.1237	+0.0336	−0.1111	−0.1031	+0.0209	+0.1265	+0.1531
8.5	+0.0939	+0.0819	−0.0650	−0.1201	−0.0339	+0.0842	+0.1429
9.0	+0.0458	+0.1063	−0.0103	−0.1121	−0.0768	+0.0353	+0.1199
9.5	−0.0079	+0.1041	+0.0408	−0.0827	−0.1017	−0.0137	+0.0859
10.0	−0.0544	+0.0785	+0.0779	−0.0395	−0.1056	−0.0555	+0.0445

TABLE 3

$$T_n(x) = \frac{2}{2n+1}\left[n S_{n-1}(x) - (n+1) S_{n+1}(x)\right]$$

x	$T_0(x)$	$T_1(x)$	$T_2(x)$	$T_3(x)$	$T_4(x)$	$T_5(x)$	$T_6(x)$
0.0	0.0000	+0.6667	0.0000	0.0000	0.0000	0.0000	0.0000
0.5	−0.3250	+0.6174	+0.1286	+0.0139	+0.0011	+0.0001	+ 0.0000
1.0	−0.6024	+0.4783	+0.2302	+0.0520	+0.0079	+0.0009	+0.0001
1.5	−0.7924	+0.2736	+0.2830	+0.1036	+0.0244	+0.0043	+0.0006
2.0	−0.8708	+0.0385	+0.2755	+0.1539	+0.0511	+0.0124	+0.0023
2.5	−0.8324	−0.1872	+0.2083	+0.1876	+0.0841	+0.0265	+0.0065
3.0	−0.6914	−0.3668	+0.0940	+0.1918	+0.1170	+0.0466	+0.0143
3.5	−0.4774	−0.4735	−0.0450	+0.1602	+0.1405	+0.0708	+0.0262
4.0	−0.2322	−0.4945	−0.1822	+0.0941	+0.1462	+0.0945	+0.0424
4.5	+0.0028	−0.4332	−0.2912	+0.0028	+0.1284	+0.1121	+0.0610
5.0	+0.1902	−0.3075	−0.3518	−0.0983	+0.0856	+0.1176	+0.0793
5.5	+0.3044	−0.1459	−0.3537	−0.1907	+0.0216	+0.1065	+0.0931
6.0	+0.3356	+0.0187	−0.2983	−0.2569	−0.0546	+0.0766	+0.0982
6.5	+0.2904	+0.1555	−0.1980	−0.2841	−0.1306	+0.0293	+0.0907
7.0	+0.1886	+0.2417	−0.0734	−0.2668	−0.1928	−0.0298	+0.0686
7.5	+0.0590	+0.2659	+0.0504	−0.2080	−0.2292	−0.0924	+0.0323
8.0	−0.0672	+0.2306	+0.1506	−0.1191	−0.2322	−0.1480	−0.0149
8.5	−0.1638	+0.1493	+0.2096	−0.0170	−0.2003	−0.1867	−0.0669
9.0	−0.2126	+0.0443	+0.2196	+0.0789	−0.1389	−0.2006	−0.1159
9.5	−0.2082	−0.0597	+0.1825	+0.1512	−0.0583	−0.1862	−0.1539
10.0	−0.1570	−0.1401	+0.1102	+0.1875	+0.0266	−0.1445	−0.1734

TABLE 4

Coefficients for Evaluating c_i for a Given Sectional-Area Curve

$$c_i = \sum_j \mathcal{A}(\xi_j)\, d_{ij}$$

ξ_j	d_{0j}	d_{1j}	d_{2j}	d_{3j}	d_{4j}	d_{5j}	d_{6j}
−0.9491	+0.0647	−0.1844	+0.2756	−0.3235	+0.3188	−0.2590	+0.1488
−0.7415	+0.1398	−0.3111	+0.2271	+0.0910	−0.4584	+0.6335	−0.4660
−0.4058	+0.1909	−0.2324	−0.2414	+0.5902	−0.2130	−0.5520	+0.7416
0	+0.2090	0	−0.5224	0	+0.7053	0	−0.8490
+0.4058	+0.1909	+0.2324	−0.2414	−0.5902	−0.2130	+0.5520	+0.7416
+0.7415	+0.1398	+0.3111	+0.2271	−0.0910	−0.4584	−0.6335	−0.4660
+0.9491	+0.0647	+0.1844	+0.2756	+0.3235	+0.3188	+0.2590	+0.1488

REFERENCES

1. Krylov, A., "A General Theory of the Oscillations of a Ship on Waves," Transactions Institution of Naval Architects, Vol. 40 (1898).

2. Cummins, W.E., "The Forces and Moments Acting on a Body Moving in an Arbitrary Potential Stream," Taylor Model Basin Report 780 (June 1953).

3. Cummins, W.E. and Thorpe, A., "A Theoretical Study of a Spheroid Moving Under a Regular Train of Waves," Taylor Model Basin Report 908 (in preparation).

4. Pond, H.L., "The Pitching Moment Acting on a Body of Revolution Moving Under a Free Surface," Taylor Model Basin Report 819 (May 1952).

5. Landweber, L., "The Axially Symmetric Potential Flow About Elongated Bodies of Revolution," Taylor Model Basin Report 761 (August 1951).

6. Watson, G.N., "A Treatise on the Theory of Bessel Functions," Cambridge University Press (1944).

7. "Tables of Spherical Bessel Functions," Mathematical Tables Project, National Bureau of Standards, Columbia University Press.(1947).

8. Lowan, A.N. et al, "Table of the Zeroes of the Legendre Polynomials for Gauss' Mechanical Quadrature Formula," Bulletin of the American Mathematical Society, Vol. 48, No. 10 (October 1942).

INITIAL DISTRIBUTION

Copies

14 Chief, BuShips, Library (Code 312)
- 5 Technical Library
- 1 Tech Asst to Chief (Code 106)
- 1 Appl Science (Code 370)
- 1 Ship Design (Code 410)
- 2 Prelim Des and Ship Protection (Code 420)
- 1 Prelim Des (Code 421)
- 1 Submarines (Code 525)
- 1 Minesweeping (Code 530)
- 1 Torpedo Countermeasures (Code 5301)

4 Chief, BuOrd, Underwater Ordnance
- 2 Code Re6
- 2 Code Re3

2 Chief, BuAer, Aero and Hydro Br

4 Chief of Nav Res
- 1 Mech Br (Code 438)
- 1 Undersea Warfare Br (Code 466)
- 1 Math Br (Code 432)
- 1 Nav Sciences Div (Code 460)

1 CO, ONR, New York, N.Y.

1 CO, ONR, Pasadena, Calif.

1 CO, ONR, San Francisco, Calif.

1 CO, ONR, Chicago, Ill.

1 CO, ONR, Boston, Mass.

1 CDR, Norfolk Naval Shipyard, UERD

1 CDR, Boston Naval Shipyard

1 CDR, Portsmouth Naval Shipyard

1 CDR, Puget Sound Naval Shipyard

1 CO, SURASDEVDET, U.S. Atlantic Fleet

1 O in C, ONR, London, England

2 CDR, USNOL
- 1 Dr. A. May

1 DIR, USNRL

3 DIR, Langley Aero Lab, Langley Field, Va.
- 1 Dr. C. Kaplan
- 1 Mr. F.L. Thompson

2 CDR, U.S. Nav Air Missile Ctr, Port Mugu, Calif.
- 1 Dr. H.A. Wagner

2 CDR, USNOTS, Underwater Ord Div, Pasadena, Calif.

2 CDR, USNOTS, Inyokern, Calif.
- 1 Dr. E.O. Cooper

1 CO, U.S. Nav Mine Countermeas Sta, Panama City, Fla.

1 CO, USNUOS, Newport, R.I.

1 CO, Frankford Arsenal Office of Air Res, Appl Mech Gp, Wright-Patterson AFB, Dayton, Ohio

3 DIR, Natl BuStand
- 1 Mr. E.V. Hobbs
- 1 Dr. G.H. Keulegan

1 Electric Boat Div, Gen Dyn Corp, Groton, Conn. Attn: F.S. Cauldwell

1 Sperry Gyroscope Co, Marine Div, Long Island, N.Y. Attn: J.H. Chadwick

1 BAR, Bendix Aviation Corp, Teterboro, N.J.

1 Library of Congress, Tech Info Div, ASTIA Ref Ctr, Wash., D.C.

1 Asst Sec of Defense (Res and Dev) DOD

1 DIR, Oak Ridge Natl Lab, Oak Ridge, Tenn.

Copies

8 ALUSNA, London, England

2 DIR, Appl Phys Lab, Johns Hopkins U., Silver Spring, Md.

1 DIR, Daniel Guggenheim Aero Lab, CIT, Pasadena, Calif.

1 DIR, Fluid Mech Lab, Columbia U, New York, N.Y.

1 DIR, Fluid Mech Lab, U of Calif, Berkeley, Calif.

3 DIR, ETT, SIT, Hoboken, N.J.
- 1 Mr. Peters
- 1 Dr. B.V. Korvin-Kroukovsky

2 DIR of Aero Res, NACA, Washington, D.C.

1 DIR, Hydro Lab, Dept of Civil & Sanitary Engin, MIT, Cambridge, Mass.

1 DIR, Exptl Nav Tank, Dept of Nav Arch & Mar Engin, Univ of Michigan, Ann Arbor, Mich.

1 DIR, Inst for Fluid Dyn & Appl Math, U of Md., College Park, Md.

1 DIR, Inst of Aero Sciences, New York, N.Y.

1 DIR, Fluid Mech Lab, NYU, New York, N.Y.

1 DIR, Ord Res Lab, Penn State Univ, State College, Pa.

1 Admin, Webb Inst of Nav Arch, Long Island, N.Y.

1 DIR, Iowa Inst of Hydraulic Res, State U of Iowa, Iowa City, Iowa

1 DIR, St. Anthony Falls Hydraulic Lab, U of Minn., Minneapolis, Minn.

1 Head, Dept of Nav Arch & Mar Engin, MIT, Cambridge, Mass.

1 Office of Tech Services, U.S. Dept of Comm, Wash, D.C.

1 Document Service Ctr, ASTIA, Dayton, Ohio

1 Editor, Engineering Index, New York, N.Y.

1 Editor, Aero Engin Review, New York, N.Y.

1 Hydro Labs, Attn: Exec Comm, CIT, Pasadena, Calif.

1 NYU Inst for Math & Mech, New York, N.Y.

1 Cornell Aero Lab, Inc., Buffalo, N.Y. Attn: Librarian

1 Reed Res, Inc., Washington, D.C. Attn: Librarian

1 Dept of Civil Engin, Colo. A & M College, Ft Collins Colo.

1 Goodyear Aircraft Corp, Akron, Ohio

1 Librarian, Amer Soc of Mech Engin, New York, N.Y.

1 Librarian, Amer Soc of Civil Engin, New York, N.Y.

1 Librarian, Franklin Inst, Philadelphia, Pa.

1 Librarian, Mech Res Library, Ill. Inst of Tech, Tech Ctr, Chicago, Ill.

1 Librarian, Pacific Aero Library, Los Angeles, Calif.

2 Tech Library, Glenn L. Martin Co, Baltimore, Md.

1 Chairman, Graduate Div of Appl Math, Brown U, Providence, R.I.

1 Dr. V.L. Streeter, Prof of Hydraulics, Dept of Civil Engin, U of Mich., Ann Arbor, Michigan

1 Prof.G. Birkhoff, Dept of Math, Harvard Univ, Cambridge,Mass.

2 Dr. J.V. Wehausen, Editor, Math Reviews, Amer Math Soc, Providence, R.I.

1 Dr. David Gilbarg, Dept of Math, Indiana Univ, Bloomington, Ind.

Copies

1 Prof. K.E. Schoenherr, Dean, School of Engin, U of Notre Dame, Notre Dame, Ind.

1 Mr. H. Ziebolz, Vice-Pres, Askania Regulator Co, Chicago, Ill.

1 Prof. M.A. Abkowitz, MIT, Cambridge, Mass.

Mr. J.P. Breslin, SIT, Hoboken, N.J.

1 Prof. N.W. Conner, North Carolina State College, Raleigh, N.C.

1 CAPT W.S. Diehl, USN, Associate Mem, Panel on Hydro of Submerged Bodies, Washington, D.C.

1 RADM P.F. Lee, USN (Ret), VP, Gibbs and Cox, Inc., New York, N.Y.

1 Dr. George C. Manning, Prof. Nav Arch, MIT, Cambridge, Mass.

1 RADM A.I. McKee, USN (Ret), Asst. Gen Mgr, Elec Boat Div, Gen Dyn Corp, Groton, Conn.

1 Prof. F.M. Lewis, MIT, Cambridge, Mass.

1 DIR, Hydro Lab, Natl Res Council, Ottawa, Canada

1 Prof. T.H. Havelock, Newcastle-on-Tyne, England

1 Mr. C. Wigley, London, England

1 Dr. Georg Weinblum, Ingenieur Schule, Hamburg, Germany

1 Supt, Nederlandsh Scheepsbouwkundig Proefstation, Haagsteeg, Wageningen, The Netherlands

1 Prof. J.K. Lunde, Skipsmodelltanken, Trondheim, Norway

1 DIR, British Shipbldg Res Assoc, London, England

1 Dr. J.F. Allan, Supt, Ship Div, Natl Phys Lab, Middlesex, England

1 Dr. J. Okaba, The Res Inst for Appl Mech, Kyushu U, Hakozaki-machi, Fukuoka-shi, Japan

1 Canadian Natl Res Establishment, Halifax, Canada

1 Admiralty Res Lab, Middlesex, England

1 CAPT R. Brard, Directeur, Bassin D'Essais des Carenes, Paris, France

1 Dr. L. Malavard, Office National d'Etudes et de Recherches Aeronautiques, Paris, France

1 Gen. Ing. U. Pugliese, Presidente, Istituto Nazionale per Studi ed Esperienze di Architettura Navale, via della Vasca Navale 89, Rome, Italy

1 Sr. M. Acevedo y Campoamor, Director, Canal de Experiencias Hidrodinamicas, Madrid, Spain

1 Dr. J. Dieudonne, Directeur, Institut de Recherches de la Construction Navale, Paris, France

1 Prof. H. Nordstrom, Director, Statens Skeppsprovning-sanstalt, Goteborg, Sweden

1 Dr. S.L. Smith, Director, British Shipbldg Res Assoc, London, England

1 Armaments Res Establishment, Hants, England

1 Editor, Bulletin of the British Hydro Res Assoc, Essex, England

9 BJSM (NS)

3 CJS

PRNC WASH D C

David W. Taylor Model Basin. Rept. 910.
HYDRODYNAMIC FORCES AND MOMENTS ACTING ON A SLENDER BODY OF REVOLUTION MOVING UNDER A REGULAR TRAIN OF WAVES, by William E. Cummins. December 1954. vi, 35 p. incl. tables, figs., refs. UNCLASSIFIED

The hydrodynamic forces and moments acting on a slender body of revolution are found for the case in which the body is moving with a constant linear velocity under a sinusoidal train of waves oblique to the course of the body. The analysis makes use of a representation of the body by a system of singularities, and the dynamic effects are evaluated. The forces and moments are given explicitly as functions of the sectional-area curve of the body. Three illustrative examples are worked out, including a case in which there is no analytic expression available for the sectional-area curve.

1. Bodies of revolution - moments
2. Water waves - Interference
3. Water waves - Physical effects
4. Bodies of revolutions - Hydrodynamic characteristics

I. Cummins, William E.

David W. Taylor Model Basin. Rept. 910.
HYDRODYNAMIC FORCES AND MOMENTS ACTING ON A SLENDER BODY OF REVOLUTION MOVING UNDER A REGULAR TRAIN OF WAVES, by William E. Cummins. December 1954. vi, 35 p. incl. tables, figs., refs. UNCLASSIFIED

The hydrodynamic forces and moments acting on a slender body of revolution are found for the case in which the body is moving with a constant linear velocity under a sinusoidal train of waves oblique to the course of the body. The analysis makes use of a representation of the body by a system of singularities, and the dynamic effects are evaluated. The forces and moments are given explicitly as functions of the sectional-area curve of the body. Three illustrative examples are worked out, including a case in which there is no analytic expression available for the sectional-area curve.

1. Bodies of revolution - moments
2. Water waves - Interference
3. Water waves - Physical effects
4. Bodies of revolutions - Hydrodynamic characteristics

I. Cummins, William E.

David W. Taylor Model Basin. Rept. 910.
HYDRODYNAMIC FORCES AND MOMENTS ACTING ON A SLENDER BODY OF REVOLUTION MOVING UNDER A REGULAR TRAIN OF WAVES, by William E. Cummins. December 1954. vi, 35 p. incl. tables, figs., refs. UNCLASSIFIED

The hydrodynamic forces and moments acting on a slender body of revolution are found for the case in which the body is moving with a constant linear velocity under a sinusoidal train of waves oblique to the course of the body. The analysis makes use of a representation of the body by a system of singularities, and the dynamic effects are evaluated. The forces and moments are given explicitly as functions of the sectional-area curve of the body. Three illustrative examples are worked out, including a case in which there is no analytic expression available for the sectional-area curve.

1. Bodies of revolution - moments
2. Water waves - Interference
3. Water waves - Physical effects
4. Bodies of revolutions - Hydrodynamic characteristics

I. Cummins, William E.

David W. Taylor Model Basin. Rept. 910.
HYDRODYNAMIC FORCES AND MOMENTS ACTING ON A SLENDER BODY OF REVOLUTION MOVING UNDER A REGULAR TRAIN OF WAVES, by William E. Cummins. December 1954. vi, 35 p. incl. tables, figs., refs. UNCLASSIFIED

The hydrodynamic forces and moments acting on a slender body of revolution are found for the case in which the body is moving with a constant linear velocity under a sinusoidal train of waves oblique to the course of the body. The analysis makes use of a representation of the body by a system of singularities, and the dynamic effects are evaluated. The forces and moments are given explicitly as functions of the sectional-area curve of the body. Three illustrative examples are worked out, including a case in which there is no analytic expression available for the sectional-area curve.

1. Bodies of revolution - moments
2. Water waves - Interference
3. Water waves - Physical effects
4. Bodies of revolutions - Hydrodynamic characteristics

I. Cummins, William E.

David W. Taylor Model Basin. Rept. 910.
HYDRODYNAMIC FORCES AND MOMENTS ACTING ON A SLENDER BODY OF REVOLUTION MOVING UNDER A REGULAR TRAIN OF WAVES, by William E. Cummins. December 1954. vi, 35 p. incl. tables, figs., refs. UNCLASSIFIED

The hydrodynamic forces and moments acting on a slender body of revolution are found for the case in which the body is moving with a constant linear velocity under a sinusoidal train of waves oblique to the course of the body. The analysis makes use of a representation of the body by a system of singularities, and the dynamic effects are evaluated. The forces and moments are given explicitly as functions of the sectional-area curve of the body. Three illustrative examples are worked out, including a case in which there is no analytic expression available for the sectional-area curve.

1. Bodies of revolution - moments
2. Water waves - Interference
3. Water waves - Physical effects
4. Bodies of revolutions - Hydrodynamic characteristics

I. Cummins, William E.

David W. Taylor Model Basin. Rept. 910.
HYDRODYNAMIC FORCES AND MOMENTS ACTING ON A SLENDER BODY OF REVOLUTION MOVING UNDER A REGULAR TRAIN OF WAVES, by William E. Cummins. December 1954. vi, 35 p. incl. tables, figs., refs. UNCLASSIFIED

The hydrodynamic forces and moments acting on a slender body of revolution are found for the case in which the body is moving with a constant linear velocity under a sinusoidal train of waves oblique to the course of the body. The analysis makes use of a representation of the body by a system of singularities, and the dynamic effects are evaluated. The forces and moments are given explicitly as functions of the sectional-area curve of the body. Three illustrative examples are worked out, including a case in which there is no analytic expression available for the sectional-area curve.

1. Bodies of revolution - moments
2. Water waves - Interference
3. Water waves - Physical effects
4. Bodies of revolutions - Hydrodynamic characteristics

I. Cummins, William E.

David W. Taylor Model Basin. Rept. 910.
HYDRODYNAMIC FORCES AND MOMENTS ACTING ON A SLENDER BODY OF REVOLUTION MOVING UNDER A REGULAR TRAIN OF WAVES, by William E. Cummins. December 1954. vi, 35 p. incl. tables, figs., refs. UNCLASSIFIED

The hydrodynamic forces and moments acting on a slender body of revolution are found for the case in which the body is moving with a constant linear velocity under a sinusoidal train of waves oblique to the course of the body. The analysis makes use of a representation of the body by a system of singularities, and the dynamic effects are evaluated. The forces and moments are given explicitly as functions of the sectional-area curve of the body. Three illustrative examples are worked out, including a case in which there is no analytic expression available for the sectional-area curve.

1. Bodies of revolution - moments
2. Water waves - Interference
3. Water waves - Physical effects
4. Bodies of revolutions - Hydrodynamic characteristics

I. Cummins, William E.

David W. Taylor Model Basin. Rept. 910.
HYDRODYNAMIC FORCES AND MOMENTS ACTING ON A SLENDER BODY OF REVOLUTION MOVING UNDER A REGULAR TRAIN OF WAVES, by William E. Cummins. December 1954. vi, 35 p. incl. tables, figs., refs. UNCLASSIFIED

The hydrodynamic forces and moments acting on a slender body of revolution are found for the case in which the body is moving with a constant linear velocity under a sinusoidal train of waves oblique to the course of the body. The analysis makes use of a representation of the body by a system of singularities, and the dynamic effects are evaluated. The forces and moments are given explicitly as functions of the sectional-area curve of the body. Three illustrative examples are worked out, including a case in which there is no analytic expression available for the sectional-area curve.

1. Bodies of revolution - moments
2. Water waves - Interference
3. Water waves - Physical effects
4. Bodies of revolutions - Hydrodynamic characteristics

I. Cummins, William E.